Local model development

Deliverable 4.3 in project Model-based Global Assessment of Hydrological Pressure (GlobalHydroPressure)

Olsson, Jonas; Sörensen, Johanna; Elenius, Maria ; Silva, Benedito; Fragoso Jr., Carlos Ruberto; Li, Hong; Beldring, Stein

2021

Document Version:
Förlagets slutgiltiga version

Local model development

Deliverable 4.3 in project Model-based Global Assessment of Hydrological Pressure (GlobalHydroPressure)

Authors: Jonas Olsson (SMHI), Johanna Sörensen (LU), Maria Elenius (SMHI), Benedito Silva (UNIFEI), Carlos Ruberto Fragoso Jr. (UFAL), Hong Li (NVE) and Stein Beldring (NVE)

Date: 2021-04-30

Contents

1. Introduction

The objective of GlobalHydroPressure is to provide global model-based support for assessing and quantifying the fundamental hydrological pressure in basins worldwide. A consistent and reliable estimation of this pressure is a prerequisite for assessment of vulnerability and resilience to the total, multiple environmental pressure, including both natural and human-driven components. The project will develop existing hydrological models on global and local scales into innovative tools for supporting the decisions of end users. Local case studies span different climatic, areal and topographic characteristics so that hydrological models may be adapted to different characteristics and may then be used to support local vulnerability, resilience and risk assessment in ungauged regions of difficult access, as well as contribute with input to practical tools for adaptation and decision support. The applications covered in the cases include e.g. water resources management, hydropower production, flood risk assessment and agricultural production. An important aspect of GlobalHydroPressure is the multi-scale perspective, as different hydro-meteorological hazards (extreme events) operate on widely different scales in time and space. Examples of extremes include flash floods, with scales down to hours and single km^2, and droughts, with scales up to multi-years and continents.

GlobalHydroPressure strives to develop tools and methods for assessing hydrological pressure worldwide through coordinated case studies in Europe, South America and Asia. These case studies cover a wide range of dimensions with respect to the nature of the hydrological pressures, required decisions by stakeholders, socioeconomic conditions and climates. The spatial extent of the different case studies ranges from a few to several to 10^6 km^2. The temporal horizons for which hydrological pressures will be assessed spans from short-term forecasting (hours to a few days) to long-term climate projections (several decades). Figure 1 visualizes the different case studies with respect to spatial scale, temporal scale and hydrological pressure. Each case study addresses location-specific hydrological risks and adaptation challenges. Nevertheless, three cross-cutting themes can be identified: (*i*) fluvial flooding and land use change (Brazil, Western Norway), (*ii*) droughts and agriculture (Sweden, Brazil, China), and (*iii*) glacier retreat and hydropower production (Norway, China). In the following, the key characteristics of each case study will be briefly described. More detailed information on each case is provided in Appendix A.

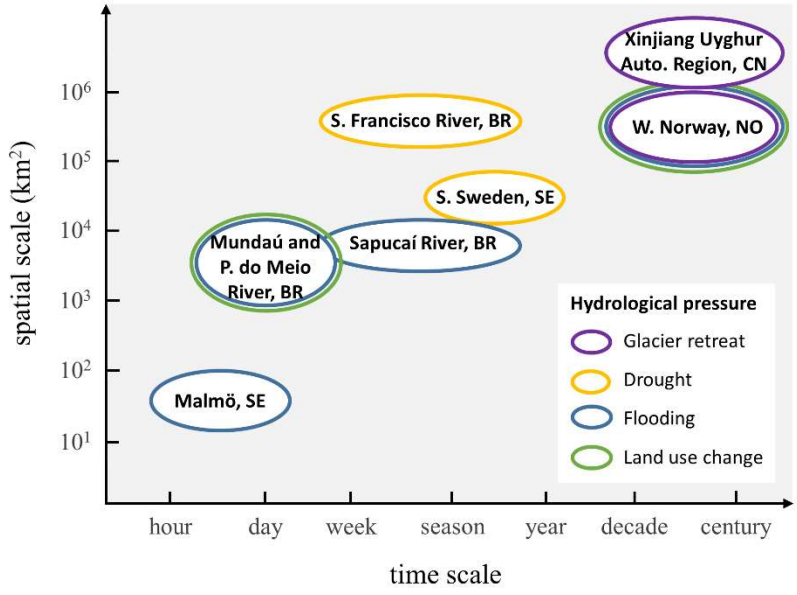

Figure 1: *Classification of the six case studies with respect to spatial scale, temporal scale and hydrological pressure*

In all case studies, local models for assessing different hydrological pressures have been developed and evaluated. In this deliverable, besides a general description of the case study and its targeted hydrological pressures, the local modelling is characterized in terms of:

- Collected observations
- Model description
- Methods used for analysis and evaluation
- Examples of results

2. Local model development

In WPs 4.2-4.6 the local models are all hydrological, i.e. simulating runoff and discharge as a function of meteorological forcing. WP4.1, however, focuses on intense rainfall and cloudbursts (with subsequent pluvial flood potential). In this case, the local modelling is represented by a high-resolution convection-permitting Regional Climate Model (RCM), which is evaluated in a domain surrounding the case study area (Malmö City, SE).

2.1 WP4.1 Malmö (SE)

1. Case study no.: 4.1
2. Location: Malmö
3. Country: Sweden
4. Domain size: 7 700 hectares
5. Case study area: 4 845 hectares

6. Description of hydrological (and other) pressures:
The Malmö (SE) case study addresses pluvial flooding events in the city of Malmö caused by heavy rainfall event which appear primarily during the late summer months (July–August). The case study seeks a better understanding of the highly non-linear relationship between extreme rainfall and pluvial flooding as well as a better understanding of climate projections on urban scale.

Situated in northern Europe (Fig. 2.1.1), Malmö has a temperate climate. Intense rainfall is most common during late summer (Gustafsson et al., 2010), when humid air from the sea reaches the warm land, while stormy weather with extreme waves and water levels is most common during autumn and winter (Hanson and Larson, 2008). The maximum hourly rainfall is 26.1 and 53.4 mm, for 10 and 100 years return period respectively (Hernebring et al., 2015). The mean annual precipitation is 605 mm.

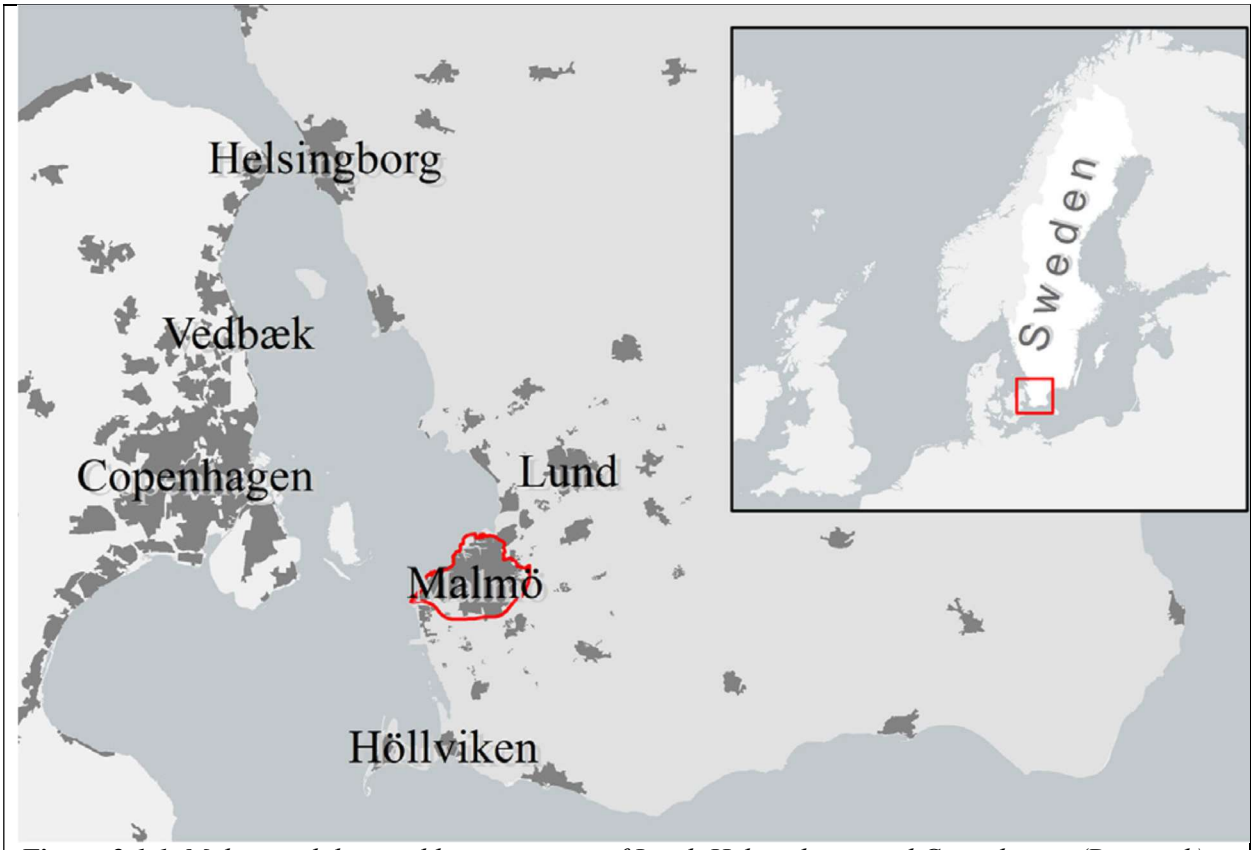

Figure 2.1.1. *Malmö and the neighbouring cities of Lund, Helsingborg, and Copenhagen (Denmark).*

The main cause behind the biggest flood events in Malmö is heavy rainfall. The main flood events appear primarily during the late summer months (July-August). In Malmö, snowmelt is not an important mechanism behind flooding.

Within the inner ring road, where the city is more densely built, 40% of the area has combined system, 7% has semi-separate system and 53% has separate system. Several areas with semi-separate system has been reconstructed to separate system during recent years. The Riseberga Brook runs from south to north in the eastern part of the city connecting to the Sege Brook short before it reaches the sea north of Malmö. Several other smaller watercourses did earlier flow through the landscape, but these have been drained in pipes.

7. Local observations collected:

Four types of precipitation data in the domain have been collected:

1. SMHI observation data: 15-min precipitation data, for the period of 1998-2018. Precipitation measured at manual and automatic measuring stations. Eight stations within the study domain.
2. PTHBV dataset: Daily precipitation data, for the period of 1998-2018. Grid data with a resolution of 4×4 km² covering the study domain.
3. VA Syd dataset: Precipitation dataset of 0.2 mm tipping bucket; for the period of 1998-2018. 33 stations within the study domain.
4. CPH observation data: 10min precipitation data at CPH airport, for the period 1966-2017.

Two datasets with flood claims have earlier been collected:

1. VA Syd dataset: Flood claims for Malmö, 1996-2015
2. Länsförsäkringar Skåne dataset: Flood claims for Region of Scania, 2000-2015

8. Model:
WP4.1 focuses on local assessment of a new very high-resolution climate mode, so-called convection permitting model (CPM), with focus on short-duration rainfall extremes. This model is named HARMONIE-AROME and from a simulation covering the Nordic region, data from a sub-domain covering southern Sweden is being analyzed. Cycle 38 of the HARMONIE-Climate regional climate modelling system (HCLIM38) are used, which is described in detail in Belušić et al. (2020).

The HCLIM38 model system provides flexibility as it contains a suite of different model configurations, each adapted for different horizontal grid resolutions. In this case study, two configurations are applied; (1) AROME which is designed for convection-permitting scales (< 4 km) and which is used with non-hydrostatic dynamics (Bengtsson et al. 2017; Seity et al. 2011; Termonia et al. 2018), and, (2) ALADIN which is the limited-area version of the global model ARPEGE used with hydrostatic dynamics, and is the default option for grid spacings $\gtrsim$ 10 km (Termonia et al. 2018). These two models are then compared with observations in order to investigate their accuracy on sub daily precipitation events.

9. Method:
The objectives of WP4.1 are to (*i*) evaluate HARMONIE-AROME in a historical period, to support the model development, and (*ii*) to assess how future changes of short-duration rainfall extremes in a CPM compares with changes as extimates from a coarser-resolution regional (RCM) or global (CPM) climate model.

In the evaluation performed, the following aspects have been included: diurnal cycle, seasonal cycle, annual maxima, amount, frequency, intensity and spatial patterns.

Extreme events were analysed based on flood claims made to the insurance company Länsförsäkringar Skåne and the water utility company VA SYD, and observed precipitation.

10. Results:
Figure 2.1.2 shows the Intensity-Duration curves of observed data and simulated data from AROME and ALADIN. For durations below 6 hours, AROME with its high spatial resolution outperforms ALADIN in comparison with observed rainfall. For 1-h duration, the bias for AROME is between -10 and +10%, while ALADIN has negative bias of up to -40% (Figure 2.1.3a). For the summer months (Figure 2.1.3b), the bias is larger for both models, but still certainly better for AROME.

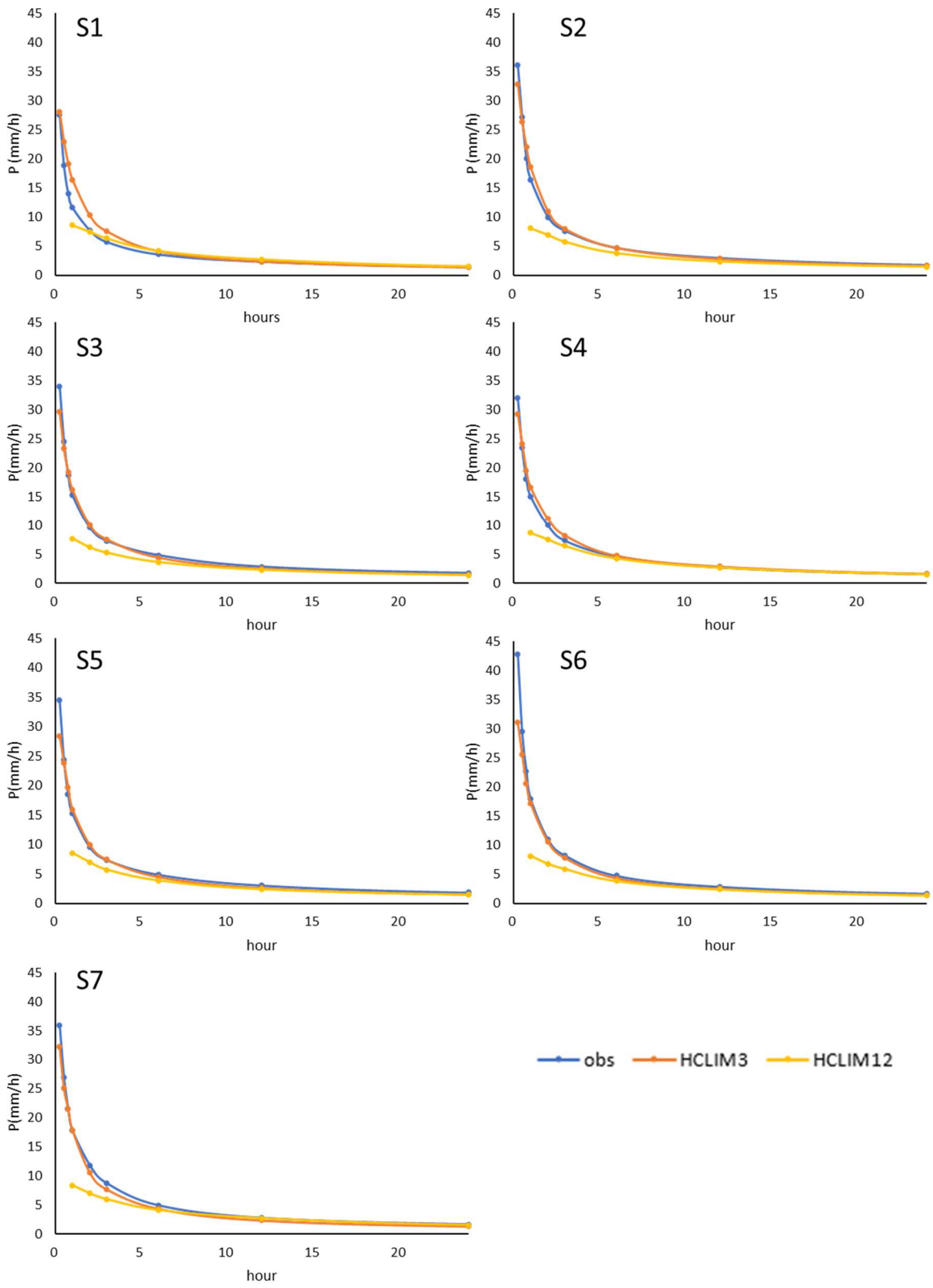

Figure 2.1.2. *Intensity-Duration curves of observed and simulated average annual maxima for the full time period.*

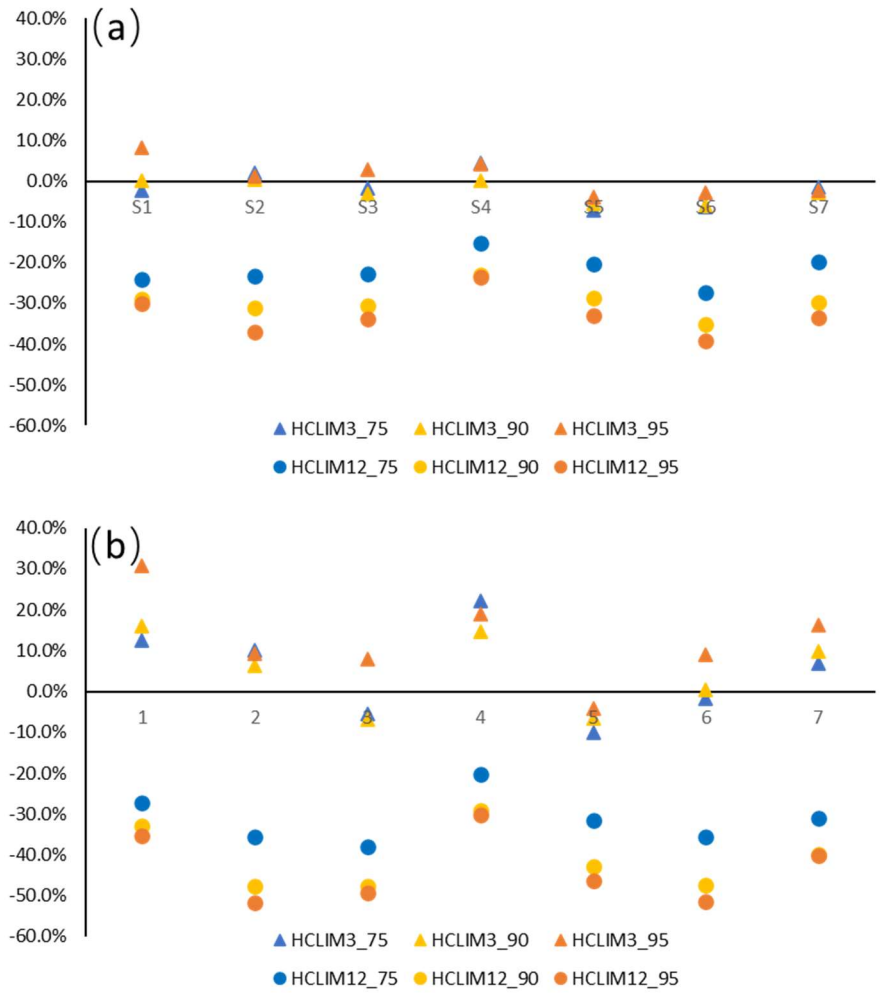

Figure 2.1.3. *Bias of percentile of 1-h precipitation I75, I90, I95. (a) in all months; (b) in summer months (JJA). Triangles denote bias of HCLIM3 (AROME), circles denote bias of HCLIM12 (ALADIN). Blue, yellow, orange denotes 75th, 90th, 95th, respectively.*

Based on flood claims collected and observed precipitation from 8 stations, extreme events were identified and categorised (category a in Table 2.1.1 below). The data were used in event-based evaluation of the AROME and ALADIN models.

Table 2.1.1. *Selected events.*

Selected events, number of flooded properties reported to LF Skåne and VA Syd, maximum precipitation during 1 h, 6 h, and 1 day (average of all stations functioning during th event), return period for 6-h precipitation, and category of event: Severe flood events (a), Other big flood events (b), Highly localised flood events (c), and Big rainfall events tha did not lead to severe flooding (d). Flood claims reported to LF Skåne before 2007 are shown in brackets, as these are considered more uncertain.

Date	Flood claims from LF Skåne [no]	Flood claims from VA Syd [no]	Max. 1-h precip. [mm]	Max. 6-h precip. [mm]	Max. 1-day precip. [mm]	Return period for 6-h precip. [years]	Category
2001-08-07	(3)	1	15.9	22.3	24.3	1.4	d
2002-08-03	(12)	75	14.6	22.8	34.4	1.5	b
2003-05-24	(35)	105	8.2	8.2	14.3	0.04	c
2003-07-18	(30)	105	19.1	30.0	32.0	3.9	b
2006-08-26	(26)	121	17.2	20.1	20.2	1.0	c
2007-07-05	169	150	10.3	39.5	70.8	10.2	a
2007-07-22	1	1	9.2	31.1	37.9	4.4	d
2008-08-24	0	0	1.3	7.2	39.0	0.03	d
2010-08-14	148	210	20.8	50.8	55.3	24.3	a
2011-06-06	26	128	13.9	15.0	15.0	0.3	c
2011-06-23	4	1	10.8	28.5	31.0	3.3	d
2012-09-25	3	4	10.0	12.2	15.7	0.2	d
2014-08-04	67*	230	17.5	19.1	27.3	0.8	b
2014-08-31	2649	2109	30.1	83.0	96.0	134.5	a

* Includes claims from 2014-08-03 as the rain fell around midnight.

2.2 WP4.2 Emån river (SE)

1. Case study no.: 4.2
2. Location: Emån River
3. Country: Sweden (southern)
4. Domain size: 4 470 km²
5. Case study area: 4 470 km²

6. Description of hydrological (and other) pressures:
The Southern Sweden case study focuses on drought and water scarcity in the Emån River basin. The region experienced an early summer drought in 2016-2017 leading to scarcity and water use restrictions. Water scarcity is unusual for the region and consequently preparedness was low. Envisaged impacts are to facilitate better decision making related to water scarcity and drought by providing tailored information and tools.

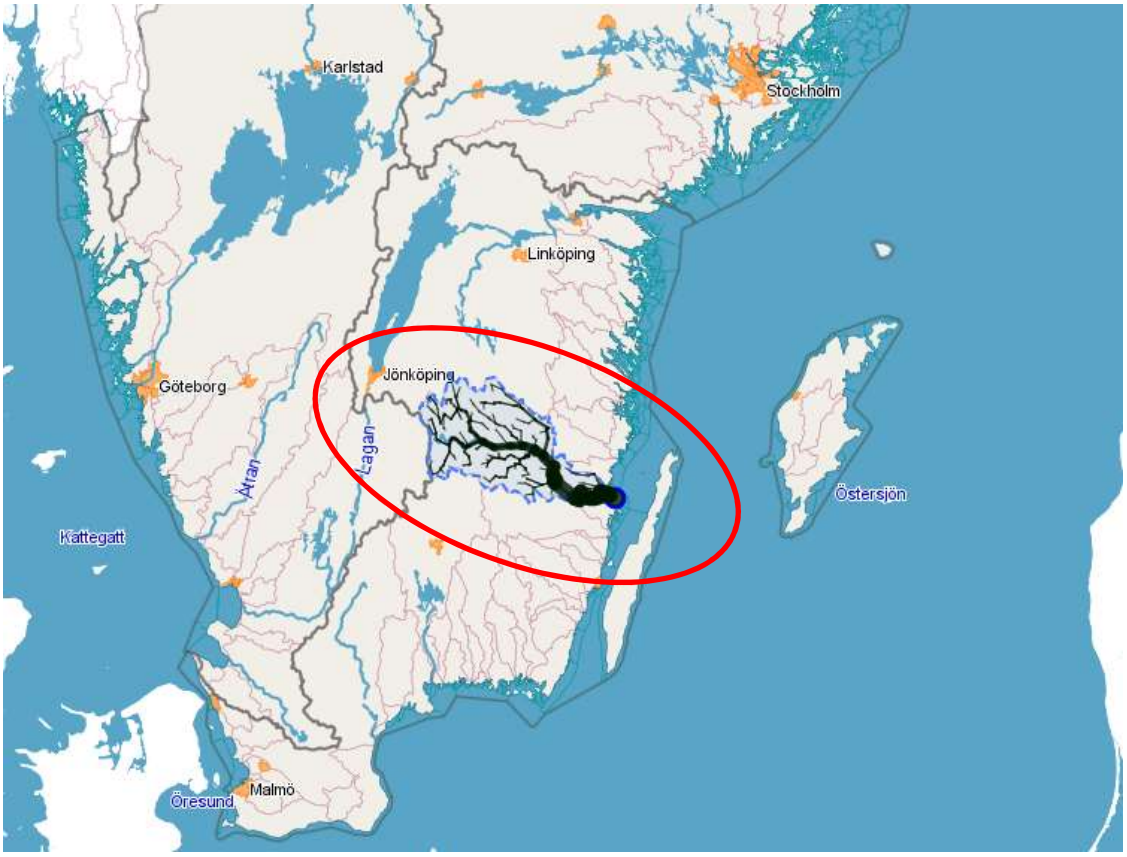

Figure 2.2.1. *The Emån river basin in south-eastern Sweden.*

7. Local observations collected:
Collection of data for WP4.2 is made through the operational monitoring network of SMHI and therefore no further collection was needed for the project.

8. Model:
HYPE is a semi-distributed rainfall-runoff model (Lindström et al., 2010). In Sweden, the S-HYPE parameterization for the model has been calibrated to simulate runoff and constituents for the entire country (approximately 40 000 sub-catchments, Strömqvist et al., 2012), using daily time-steps as default. Forcing is from the national gridded model "PTHBV". Development and recalibrations of S-HYPE during the past decade has provided continuous improvements for water flow and transport. The calibration is performed with respect to combinations of land use and soil type, apart from information

on crops. Seasonal regulations due to hydropower are also included. The focus of flow calibration has been on mean flow, which is very well described, whereas extreme flows are not fully captured.

The Emån catchment is an extraction of the S-HYPE model, including 327 sub-catchments, of which 120 have outlet lakes. There are 12 flow observation stations in the catchment. The most common land use is coniferous forest, and the most common soil is moraine.

9. Method:

Planned developments this year outside the scope of this project are to include irrigation and to include weekly regulations in S-HYPE. Both of these actions are expected to give enhanced possibilities to capture extreme low flows, and therefore to perform better seasonal forecasts of low flows. In the scope of GHP, we then aim to continue the development of improved seasonal forecasts of drought for Sweden which started in 2020, including a more detailed analysis for the Emån catchment. Different methods will be compared, e.g. ensemble streamflow predictions using ensembles of past years' precipitation and temperature (with or without the use of analogue years), and by applying meteorological seasonal forcing. The results from these hindcasts will also be compared to drought events in southern Sweden reported in the media, for which a list was compiled as part of this project.

10. Results:

The volume error for the majority of stations is very small; between -10 and +10 % (Figure 2.2.2). A few stations have larger under- and overestimates of the mean flow.

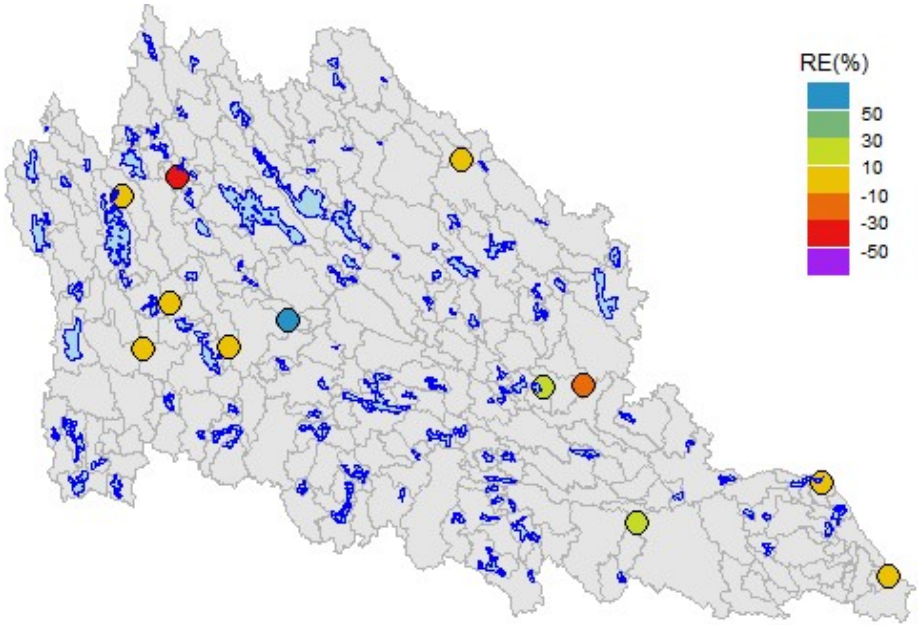

Figure 2.2.2. *The Emån catchment with marked lakes and observation stations.*

Figure 2.2.3 shows that although the flow in general is well captured by the model, the extreme event of interest here occurred earlier in the simulations than in observations, and the calculated minimum flow was too high (4.8 m^3/s instead of 2.8 m^3/s).

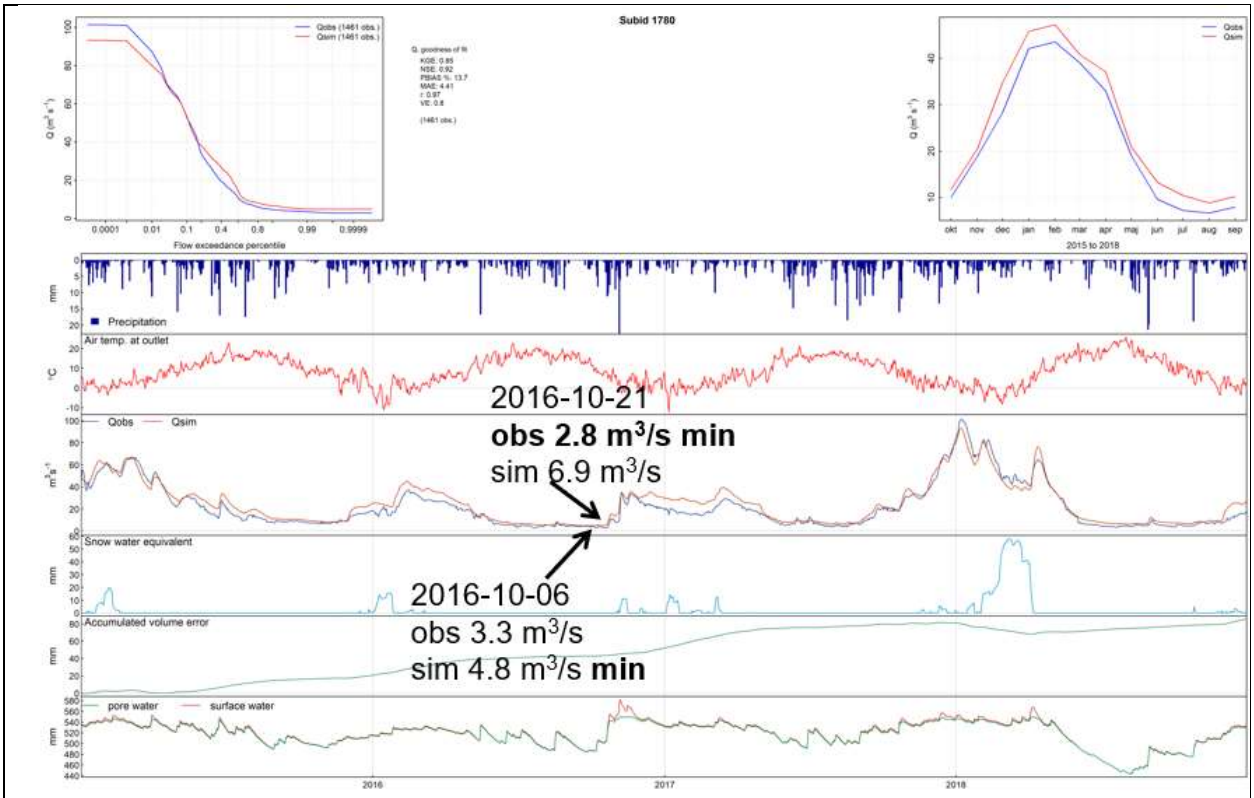

Figure 2.2.3. *The minimum flow near the outlet to the sea during the period of interest (the dry summers of 2016-2018) is marked with arrows. Here, "obs" is observation, "sim" is simulation and "min" is the minimum flow in the period shown.*

2.3 WP4.3 Rivers São Francisco and Sapucaí (BR)

1. Case study no.: 4.3.1
2. Location: Minas Gerais State
3. Country: Brazil
4. Domain size: 9,400 km²
5. Case study area: Sapucaí river basin

6. Description of hydrological (and other) pressures:
The Sapucaí River Basin is part of the Upper Paraná River Basin. It rises from the top of Mantiqueira Mountains at an altitude of 1,650 m and is divided into three parts: Upper Sapucaí, which is located from Campos do Jordão to Wenceslau Braz city; Middle Sapucaí, which extends from the city of Wenceslau Braz to the municipality of Pouso Alegre; and Lower Sapucaí, situated between the city of Pouso Alegre until it flows into the Furnas dam (Fig. 2.3.1).

The climate in the basin region has monsoon characteristics, that is, it has a dry and a humid season. In the wet season the main atmospheric systems that are associated with high accumulation of precipitation are the South Atlantic Convergence Zone (ZCAS) and the Frontal Systems (SF).
The persistence of these systems for a long period can cause, in addition to high accumulated rainfall, river floods and landslides.

In recent years, after 2012, low rainfall volumes have led to prolonged drought periods, which have resulted in significant losses to the region's economy. In addition, flash flooding and urban flooding due to very intense and localized rainfall are a major concern for the populations of the cities within the basin in recent years (Figure 2.3.2). The Basin also faces problems with unbridled human occupation

due to urbanization and the loss of water quality. To minimize these impacts, environmental services have been implemented to treat domestic and industrial effluents, as well as spring protection programs.

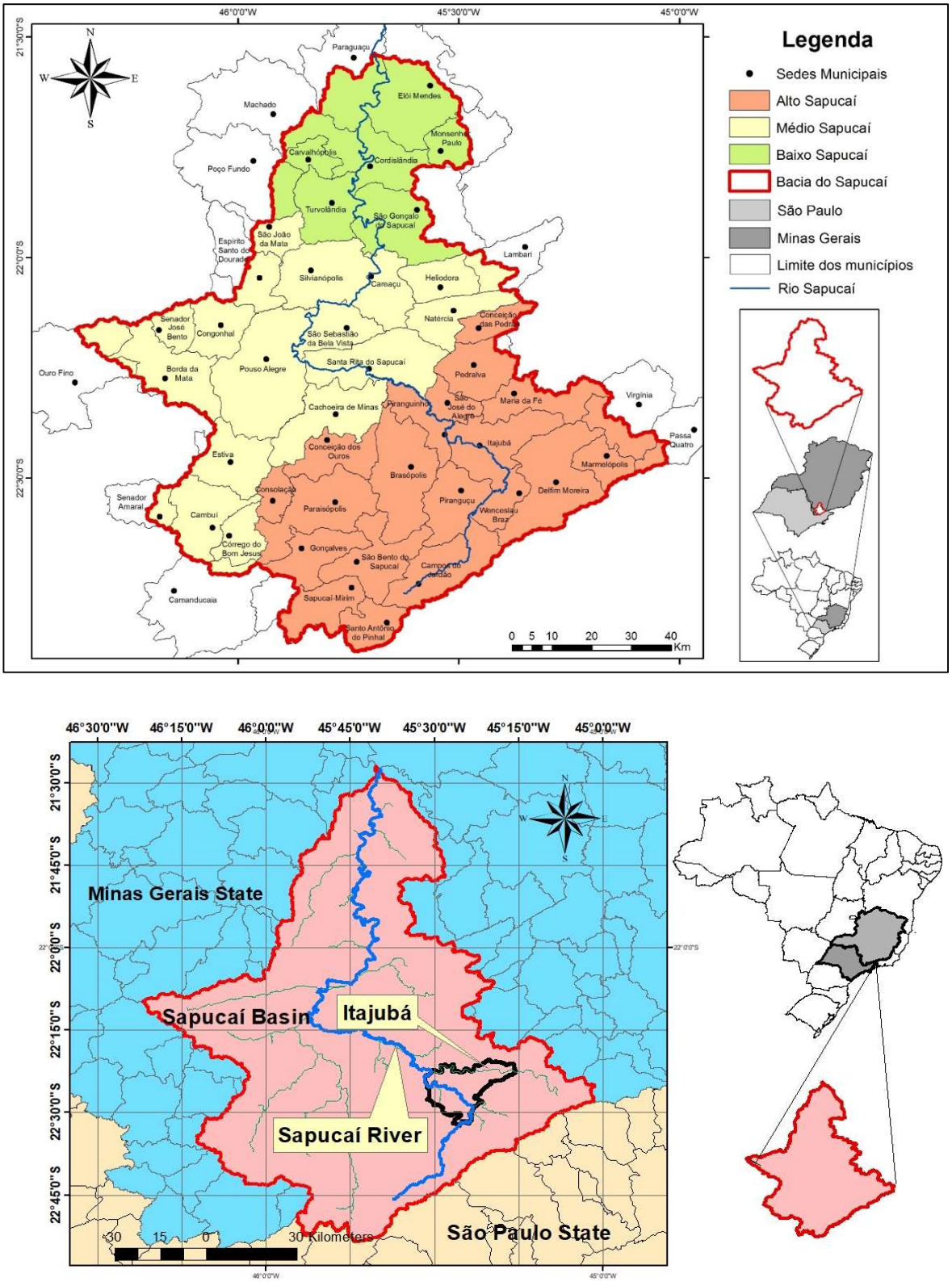

Figure 2.3.1. *Sapucaí river basin.*

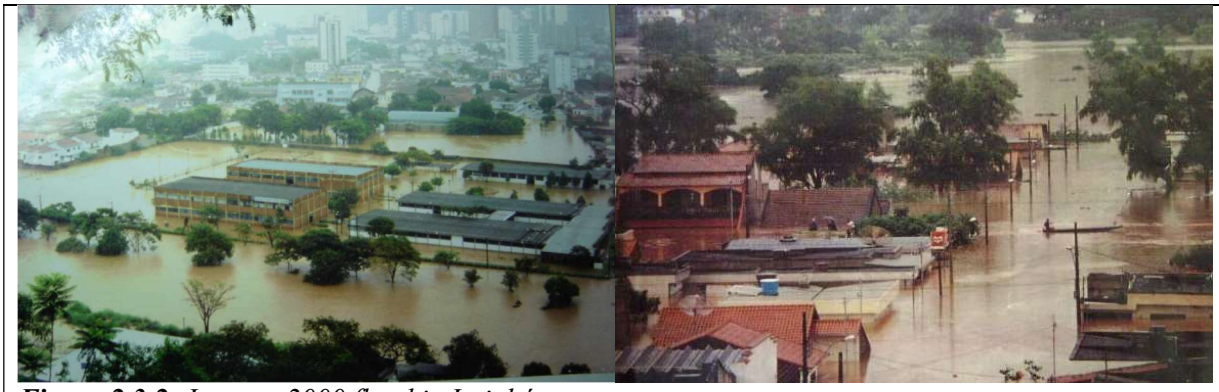

Figure 2.3.2. *January 2000 flood in Itajubá.*

7. Local observations collected:

Discharge data from hydrologic stations of the National Water Agency – ANA (http://www.snirh.gov.br/hidroweb/apresentacao) with available data since 1980 were considered to include the analysis of historical events. In addition, the spatial distribution of the stations was analysed in order to cover the entire drainage network of the basin. Therefore, a total of 14 hydrologic stations with daily time series were selected for the Sapucaí river basin.

To select the rainfall stations, the procedure was similar to the discharge stations, i.e., availability of daily data, the spatial distribution in the basin and only the stations that had rainfall data available since 1980 were chosen. In the Sapucaí River basin, 31 rainfall stations were selected.

To adjust the MGB model, data of air temperature, relative humidity, wind speed, atmospheric pressure and solar radiation or sunlight are required. However, daily climatological data available for the regions were not sufficient. Hence, data from the climatological normals provided by the National Meteorological Institute - INMET were used. In this case, a total of 10 stations was selected with data for the Sapucaí.

8. Model:

The Large Basin Hydrological Model (MGB-IPH), developed by Collischonn (2001), is a semidistributed process-based model using physical and conceptually based equations to simulate continental hydrological cycles. It was applied with success in several Brazilian basins with different characteristics. In the current version of the MGB-IPH model, the basin is divided into small unit-catchments, and then further into hydrological homogeneous regions termed hydrological response units (HRUs), generally defined from a combination of soil and vegetation type maps. Each unit-catchment has a unique river reach, where the river routing processes is performed (Figure 2.3.3). Vertical water and energy budgets are computed independently for each HRU in each unit-catchment. Soil water balance is computed considering only one soil layer. Precipitation (P) is assumed to be stored on the surface of the vegetation until maximum interception storage capacity is reached, which is determined for each HRU based on the vegetation leaf area index. Energy budget and evapotranspiration from soil, vegetation and canopy to the atmosphere is estimated by the PenmanMonteith equation.

Soil infiltration and runoff are computed based on the variable contributing area concept of the ARNO model. Subsurface flow is computed using an equation similar to the Brooks and Corey unsaturated hydraulic conductivity equation. Percolation from soil layer to groundwater is calculated according to a simple linear relation between soil water storage and maximum soil water storage. Then, the flow generated within each unit-catchment is routed to the stream network using three linear reservoirs (baseflow, subsurface flow and surface flow). Originally in the MGB-IPH model the drainage network flow routing was calculated using the linear Muskingum-Cunge method, but there are versions using

hydrodynamic and inertial routing (COLLISCHONN et al., 2007; PAIVA et al., 2011, PONTES et al., 2017).

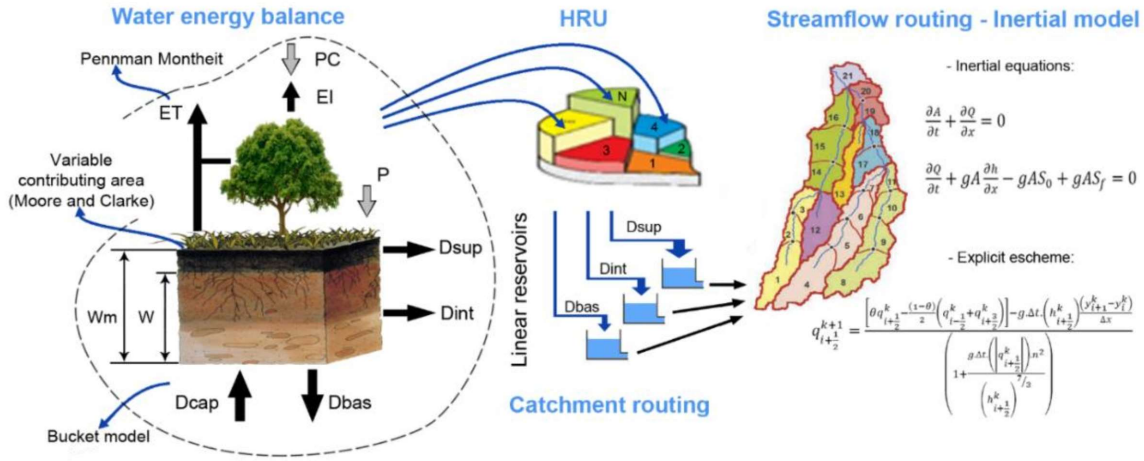

Figure 2.3.3. *MGB-IPH model structure. Source: Pontes et al. (2017).*

The soil map was digitized based on the RADAM Brasil project, which is on the 1: 1,000,000 scale. Subsequently, the map was reclassified and the soils were grouped according to the potential of runoff (Figure 2.3.4a), being considered soil that has low potential for runoff generation (A), soil with medium potential for runoff generation (B) and, finally, soil with high potential for generating runoff (C).
The land use and occupation map (Figure 2.3.4b)was elaborated through multispectral classification, opting for the supervised classification method. For this process, images were obtained from the Landsat 5 satellite, with dates of 2010 and 2011 and resolution of 30 meters, obtained from the database of the National Institute for Space Research (INPE). With the soil type and land use maps, the HRU's map shown in Figure 2.3.5a was obtained.

Discretization is the division of the basin into mini-basins, to better describe the spatial variability of processes and input variables. This is necessary because the MGB is a distributed type model. Then, the Sapucaí basin was discretized based on the digital elevation model of the terrain SRTM, with a resolution of 90 meters, made available by the Brazilian Agricultural Research Corporation – EMBRAPA (Figure 2.3.5b). Figure 2.3.6a shows the result of the discretization of the basin in a total of 229 unit-cachments. The fluviometric stations were used as the exutory of each sub-basin, so a map with 14 sub-basins was generated (Figure 2.3.6b).

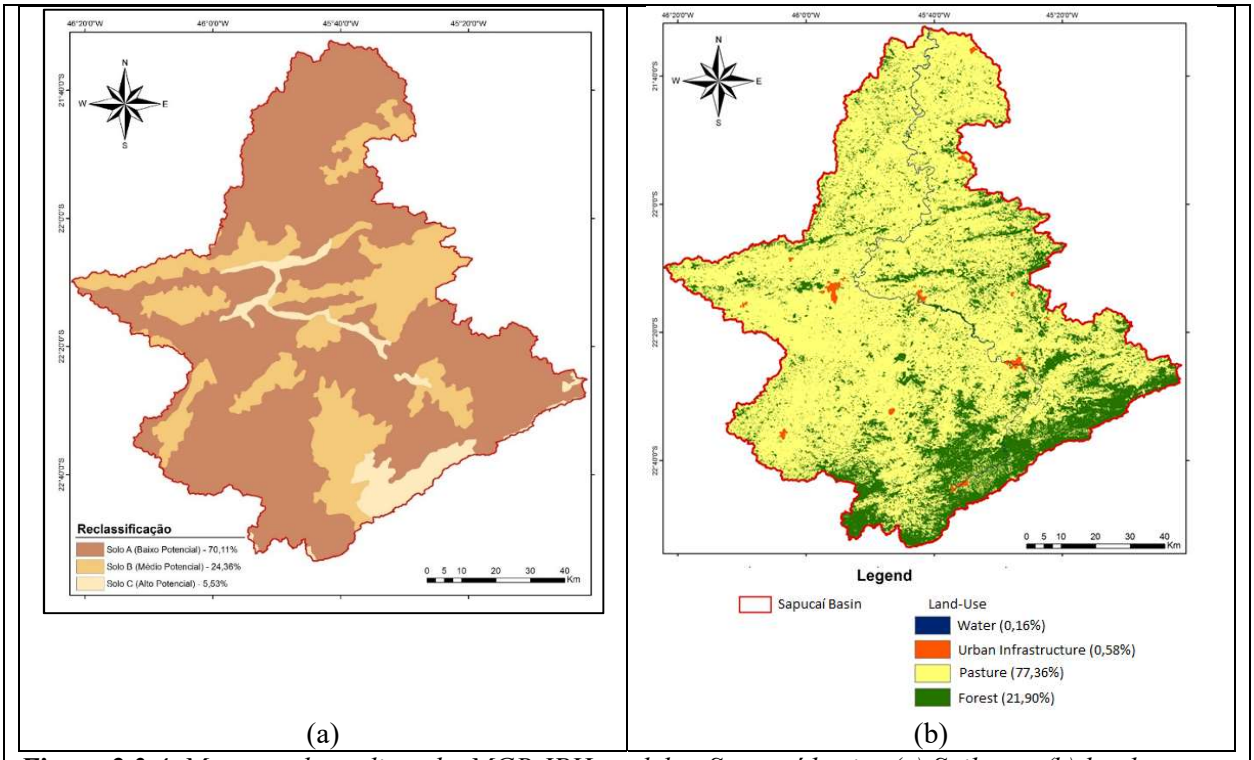

(a) (b)

Figure 2.3.4. *Maps used to adjust the MGB-IPH model to Sapucaí basin: (a) Soil map (b) land use map.*

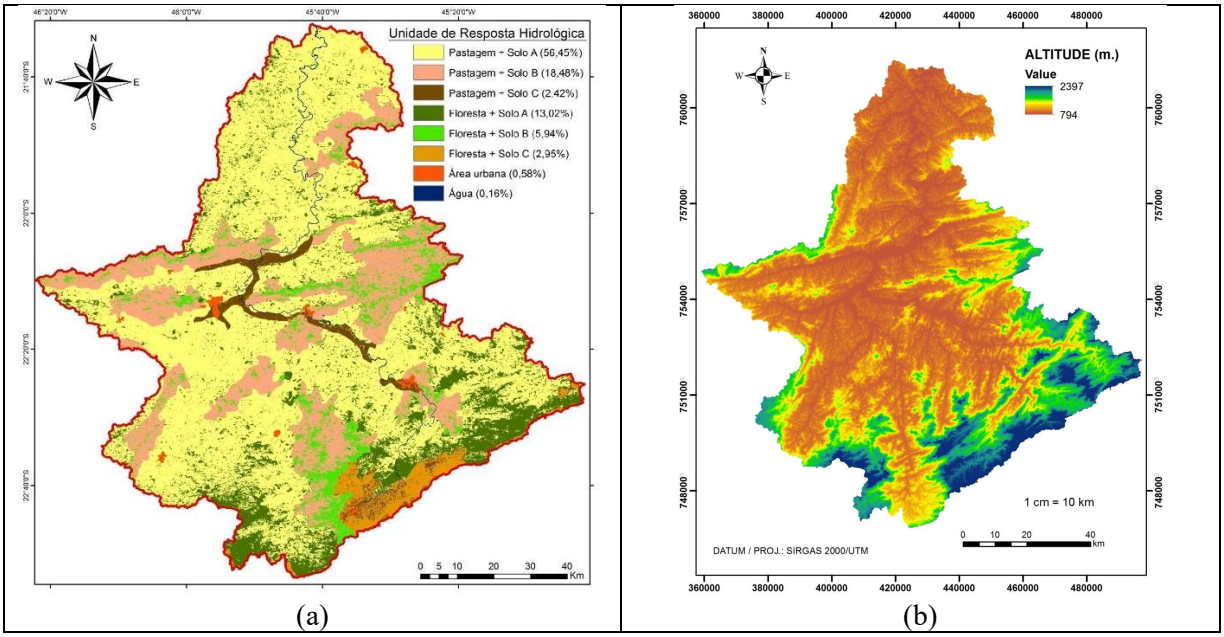

(a) (b)

Figure 2.3.5. *Maps used to adjust the MGB-IPH model o Sapucaí basin: (a) HRU map (b) relief map.*

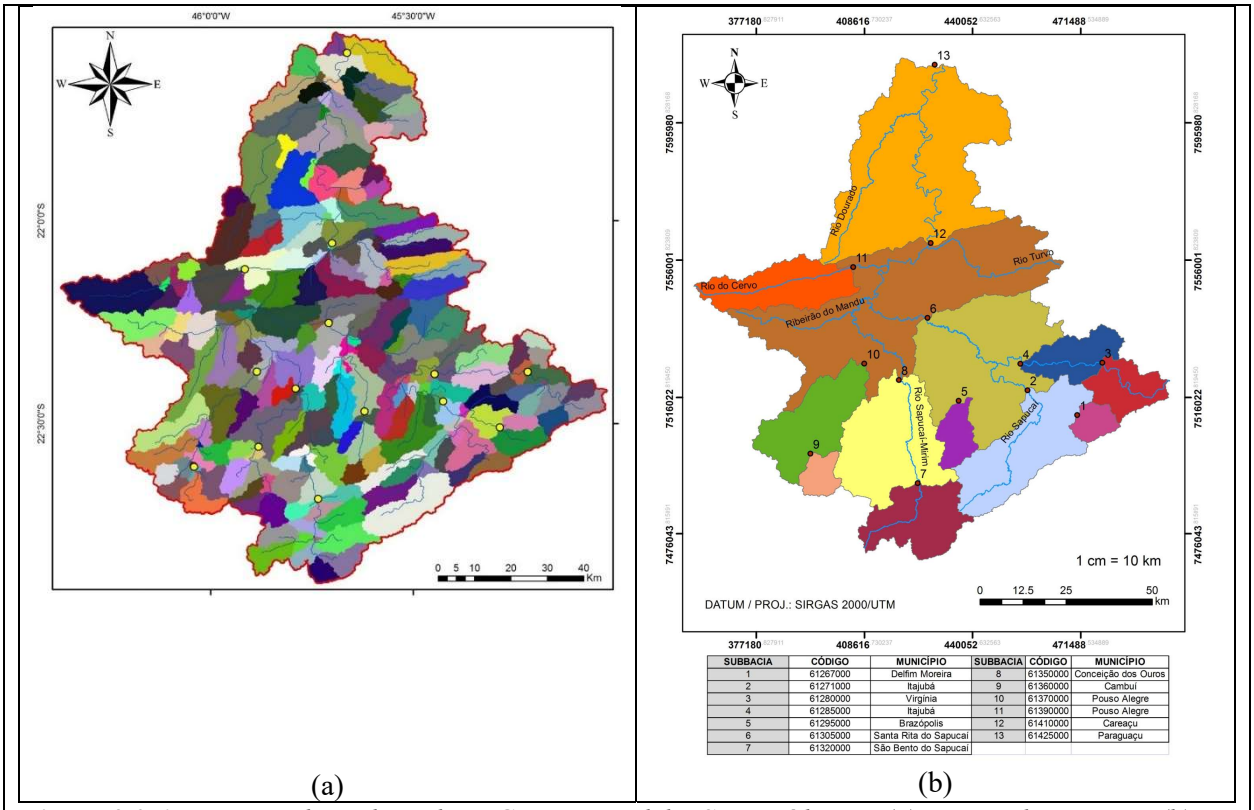

SUBBACIA	CÓDIGO	MUNICÍPIO	SUBBACIA	CÓDIGO	MUNICÍPIO
1	61267000	Delfim Moreira	8	61350000	Conceição dos Ouros
2	61271000	Itajubá	9	61360000	Cambuí
3	61280000	Virgínia	10	61370000	Pouso Alegre
4	61285000	Itajubá	11	61390000	Pouso Alegre
5	61295000	Brazópolis	12	61410000	Careaçu
6	61305000	Santa Rita do Sapucaí	13	61425000	Paraguaçu
7	61320000	São Bento do Sapucaí			

Figure 2.3.6. *Maps used to adjust the MGB-IPH model o Sapucaí basin: (a) unit-cachment map (b) sub-basin map.*

Table 2.3.1. *Sub-basins used to adjust the MGB-IPH model to the Sapucaí river.*

STATION CODE	NUMBER	AREA (km²)	RIVER
61267000	1	112	Taboão
61271000	2	869	Sapucai
61280000	3	268	Lourenço Velho
61285000	4	560	Lourenço Velho
61295000	5	156	Vargem Grande
61305000	6	2810	Sapucai
61320000	7	475	Sapucaí-mirim
61350000	8	1332	Sapucai-mirim
61360000	9	116	Itaim
61370000	10	676	Itaim
61390000	11	486	Cervo
61410000	12	7330	Sapucai
61425000	13	9410	Sapucai

9. Method:
The calibration of the MGB-IPH model for the Sapucaí river basin was performed, initially, with a manual approach, followed by an automatic multi-objective calibration, based on the genetic algorithm technique. The model was calibrated considering flow data measured between January of 1980 and December of 1989. Subsequently, to assess the quality of the adjustment, three statistical coefficients were considered: Nash-Sutcliffe (NS), Nash-Sutcliffe of logarithms (Nslog) and volume error (ΔV).

10. Results:
The results, in general, were satisfactory for most of the sub-basins, with the Nash-Sutcliffe and Nash-Sutcliffe coefficients of logarithms close to or greater than 0.70 (Table 2.3.2). For some sub-basins that had a smaller drainage area, the adjustment was below, considering the Nash-Sutcliffe values, due to the small drainage areas, which makes it difficult to adjust the model. In Figures 2.3.7 to 2.3.9 some results are presented, to show de performance for January 2000 flood, the biggest flood in the last 30 years.

Table 2.3.2. *results of MGB-IPH model calibration (1980 – 1990)*

Station (number - name)	***NS***	***NS_{log}***	***ΔV (%)***
1 - Delfim Moreira	0.246	0.064	21.589
2 - Itajubá	0.768	0.813	1.493
3 - Bairro Santa Cruz	0.338	0.381	-16.581
4 - São João de Itajubá	0.669	0.69	-8.156
5 - Brazópolis	0.825	0.818	0.032
6 - Santa Rita do Sapucaí	0.669	0.81	0.04
7 - São Bento do Sapucaí	0.263	0.078	21.214
8 - Conceição dos Ouros	0.712	0.719	9.147
9 - Cambuí	0.516	0.605	-13.799
10 - Ponte do Rodrigues	0.81	0.753	-3.072
11 - Vargem do Cervo	0.835	0.864	0.004
12 - Careaçu	0.76	0.86	-9.118
13 - Paraguaçu	0.715	0.774	15.922

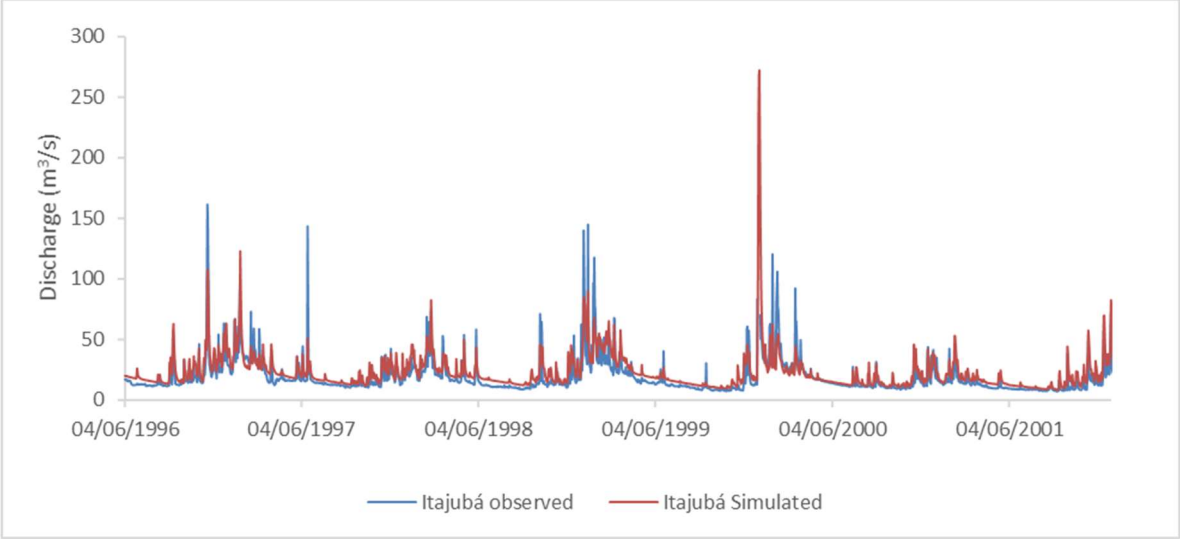

Figure 2.3.7. *MGB-IPH adjusted for Itajubá station (sub-basin 2).*

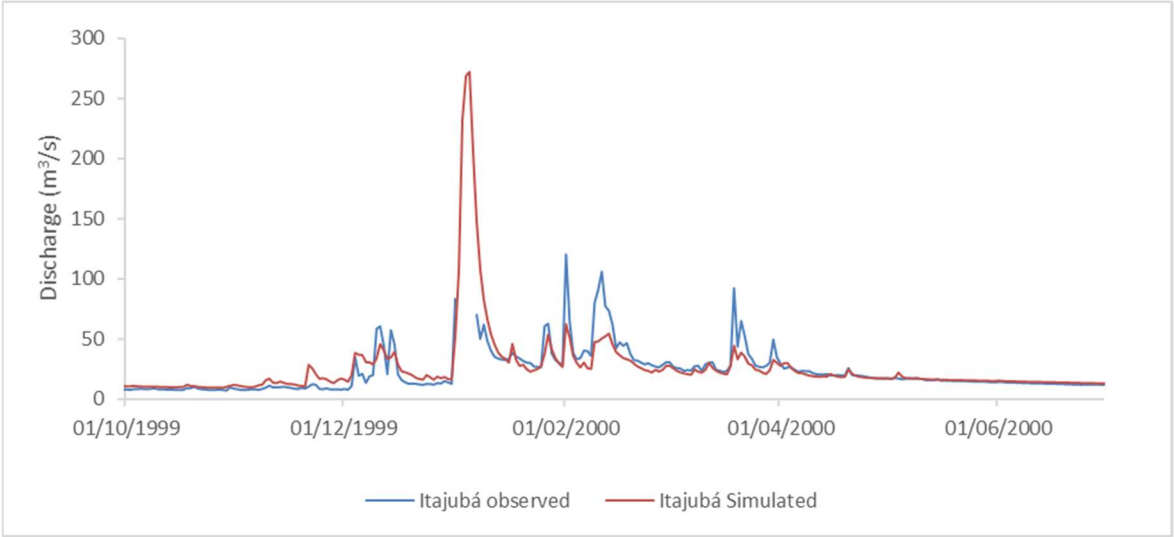

Figure 2.3.8. *MGB-IPH adjusted for Itajubá station (sub-basin 2). Detail for the January 2000 flood.*

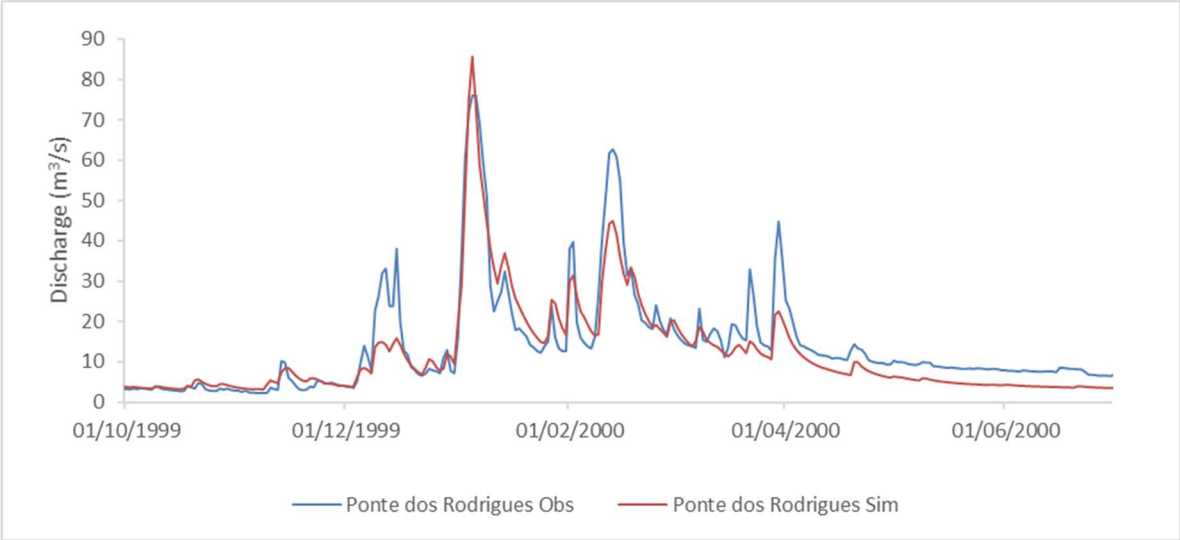

Figure 2.3.9. *MGB-IPH adjusted for Ponte do Rodrigues station (sub-basin 10). Detail for the January 2000 flood.*

1. Case study no.: 4.3
2. Location: Minas Gerais and other Brazilians Northeast States
3. Country: Brazil
4. Domain size: 639,219 km²
5. Case study area: São Francisco river basin

6. Description of hydrological (and other) pressures:

The São Francisco Basin has a large territorial extension, occupying an area covering 6 States and the Federal District. Due to the great variability of physical and climatic characteristics, the basin is divided into four parts, namely: Upper São Francisco, located in the mountainous area where the river rises in the Serra da Canastra; Middle São Francisco, located west of the state of Bahia, this being the largest division; São Francisco Sub-Middle, which lies on the border of the states of Bahia and Pernambuco and extends to the state of Alagoas; Lower São Francisco, located on the border of the states of Alagoas and Sergipe, flowing into the Atlantic Ocean (Fig. 2.3.10).

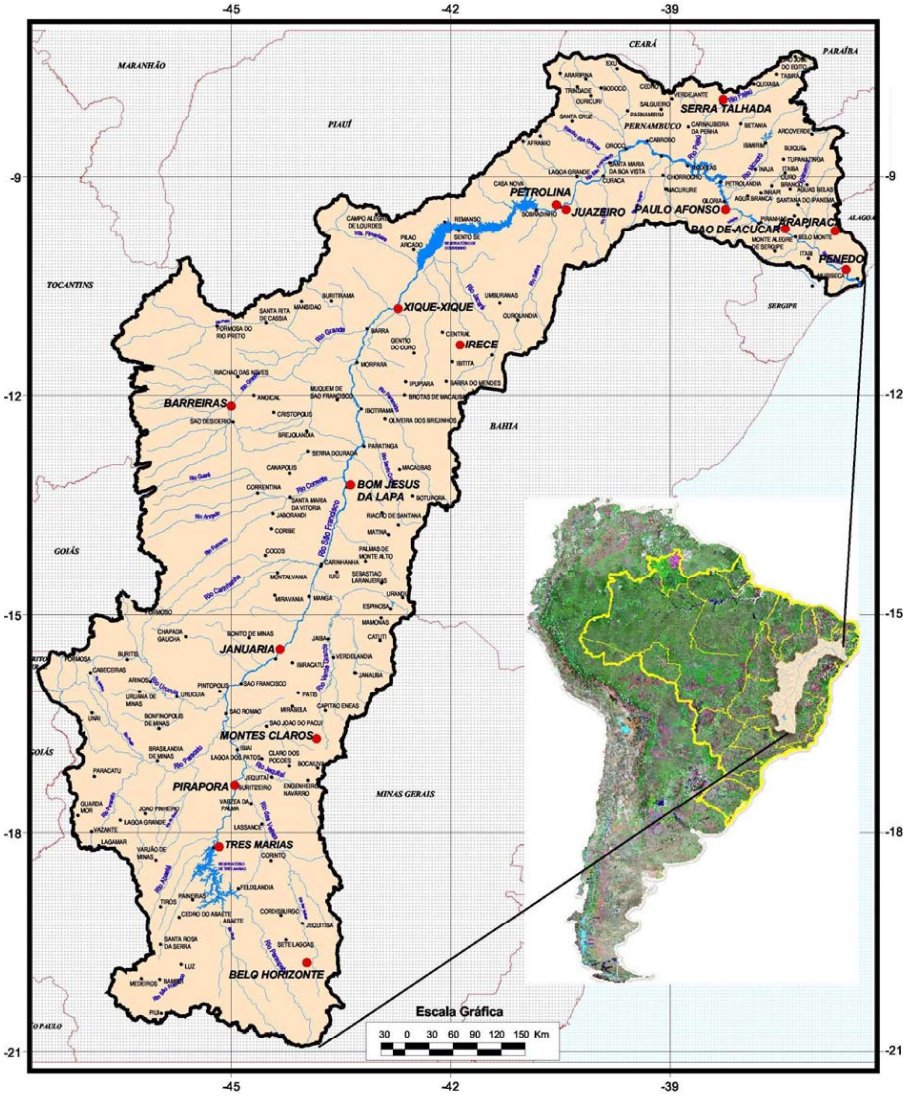

Figure 2.3.10. *São Francisco river basin (ANA, 2003).*

Due to its territorial extension, precipitation in the Basin is influenced by several meteorological systems, namely: South Atlantic Convergence Zone (ZCAS); High Level Cyclonic Vortices (VCAN); Frontal Systems (SF); Intertropical Convergence Zone (ZCIT); and Eastern Disorders (DL).

Its climate is defined by two distinct seasons, one dry and one rainy, with temperatures between 18ºC and 27ºC and little cloudiness. Its climate variability is associated with the transition from a humid and humid climate present in the Alto São Francisco region to an arid and semi-arid climate in the Sub-Middle São Francisco region. Low cloudiness and high temperature significantly increase potential evapotranspiration, which if not compensated for by rainfall can cause an imbalance in water balance. Moreover, much of the basin is within the region demarcated as a drought polygon, which according to Brazilian law is a region more susceptible to prolonged periods of drought and comprises the north of Minas Gerais and the Northeast region of Brazil.

With regard to the water use of the Basin, an important growing sector is irrigated agriculture, mainly present in the Upper, Middle and Sub-Middle São Francisco. Another important sector is hydroelectric power generation, having several hydroelectric plants along its extension. As many Brazilian states are dependent on the São Francisco Basin for different water uses, knowing their hydrological behavior is extremely important to assist in decision making.

7. Local observations collected:

Discharge data from hydrologic stations of the National Water Agency – ANA (http://www.snirh.gov.br/hidroweb/apresentacao) with available data since 1980 were considered to include the analysis of historical events. In addition, the spatial distribution of the stations was analysed in order to cover the entire drainage network of the basin. Therefore, a total of 27 hydrologic stations were selected for the São Francisco basin.

To select the rainfall stations, the procedure was similar to the discharge stations, i.e., vailability of data, the spatial distribution in the basin and only the stations that had rainfall data available since 1980 were chosen. In the São Francisco River basin, 228 rainfall stations were selected.

To adjust the MGB model, data of air temperature, relative humidity, wind speed, atmospheric pressure and solar radiation or sunlight are required. However, daily climatological data available for the regions were not sufficient. Hence, data from the climatological normals provided by the National Meteorological Institute - INMET were used. In this case, a total of 26 stations was selected with data for the São Francisco basin.

8. Model:

The Large Basin Hydrological Model (MGB-IPH), developed by Collischonn (2001), is a semidistributed process-based model using physical and conceptually based equations to simulate continental hydrological cycles. It was applied with success in several Brazilian basins with different characteristics. In the current version of the MGB-IPH model, the basin is divided into small unit-catchments, and then further into hydrological homogeneous regions termed hydrological response units (HRUs), generally defined from a combination of soil and vegetation type maps. Each unit-catchment has a unique river reach, where the river routing processes is performed (Figure 2.3.10). Vertical water and energy budgets are computed independently for each HRU in each unit-catchment. Soil water balance is computed considering only one soil layer. Precipitation (P) is assumed to be stored on the surface of the vegetation until maximum interception storage capacity is reached, which is determined for each HRU based on the vegetation leaf area index. Energy budget and evapotranspiration from soil, vegetation and canopy to the atmosphere is estimated by the PenmanMonteith equation.

Soil infiltration and runoff are computed based on the variable contributing area concept of the ARNO model. Subsurface flow is computed using an equation similar to the Brooks and Corey unsaturated hydraulic conductivity equation. Percolation from soil layer to groundwater is calculated according to a simple linear relation between soil water storage and maximum soil water storage. Then, the flow generated within each unit-catchment is routed to the stream network using three linear reservoirs (baseflow, subsurface flow and surface flow). Originally in the MGB-IPH model the drainage network flow routing was calculated using the linear Muskingum-Cunge method, but there are versions using

hydrodynamic and inertial routing (COLLISCHONN et al., 2007; PAIVA et al., 2011, PONTES et al., 2017).

The soil map was digitized based on the RADAM Brasil project, which is on the 1: 1,000,000 scale. Subsequently, the map was reclassified and the soils were grouped according to the potential of runoff (Figure 2.3.11 and Table 2.3.3), being considered soil that has low potential for runoff generation and soil with high potential for generating runoff.

The land use and occupation map (Figure 2.3.12) was elaborated through multispectral classification, opting for the supervised classification method. For this process, images were obtained from the Landsat 5 satellite, with dates of 1986 and 2001 and resolution of 30 meters, obtained from the database of the National Institute for Space Research (INPE).

Discretization is the division of the basin into regular cells, to better describe the spatial variability of processes and input variables. This is necessary because the MGB is a distributed type model. Then, the Sapucaí basin was discretized based on the digital elevation model of the terrain SRTM, with a resolution of 90 meters, made available by the Brazilian Agricultural Research Corporation – EMBRAPA (Figure 2.3.12). Figure 2.3.13 shows the result of the discretization of the basin in a total of 2502 cells. The fluviometric stations were used as the exutory of each sub-basin, so a map with 27 sub-basins was generated (Figure 2.3.13).

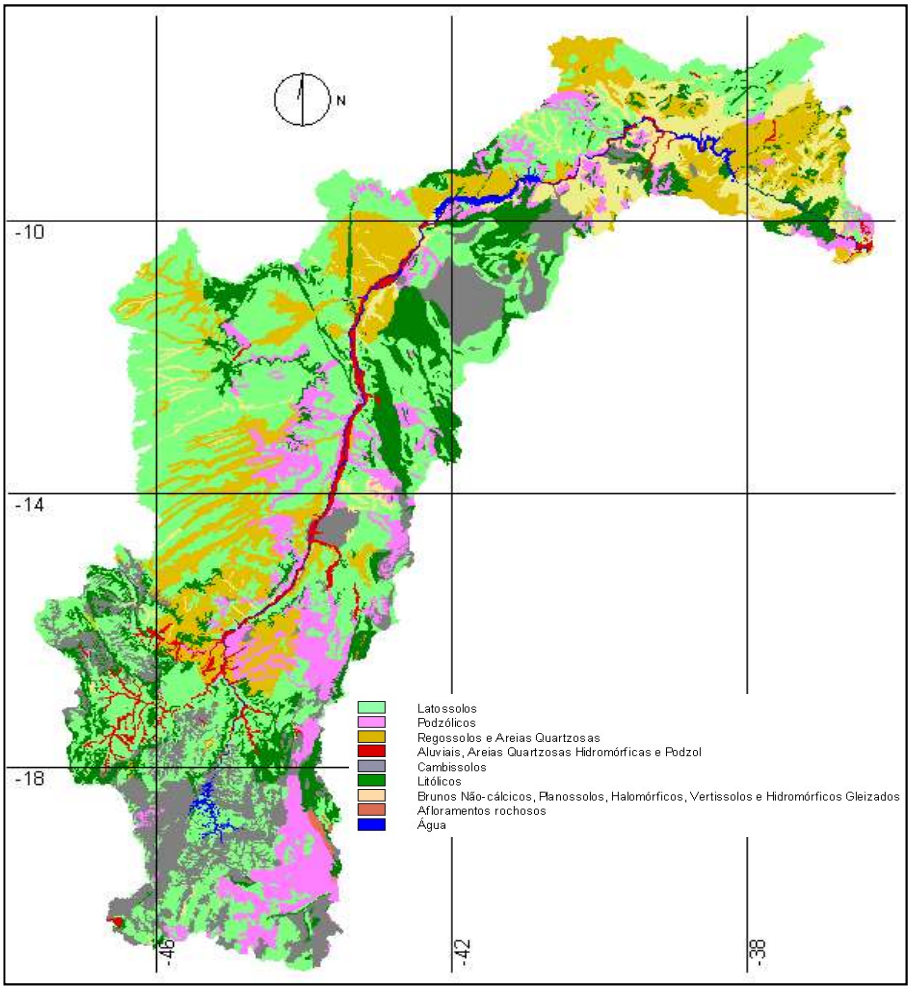

Figure 2.3.11. *Soil map used to adjust the MGB-IPH model to São Francisco basin.*

Table 2.3.3. *Area occupied by the main classes of land-use in the São Francisco basin.*

Group	Name	Area (%)
1	Latossolos	37,93
2	Podzólicos	10,65
3	Regossolos e Areias Quartzosas	16,40
4	Aluviais, Areias Quartzosas Hidromórficas e Podzol	2,17
5	Cambissolos	11,96
6	Litólicos	12,45
7	Brunos Não-cálcico, Planossolos, Halomórficos, Vertissolos e Hidromórficos Gleizados	7,24
8	Afloramentos Rochosos	0,16
9	Água	1,03

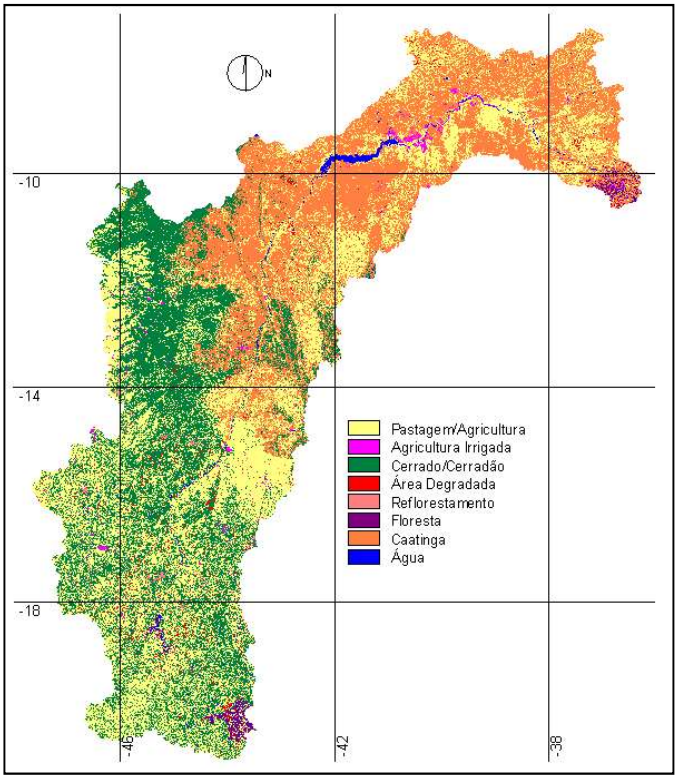

Figure 2.3.12. *Land-use map used to adjust the MGB-IPH model to São Francisco basin.*

Table 2.3.4. *Area occupied by the main classes of land-use in the São Francisco basin.*

Número	Classe	Área (%)
1	Pastagem/Agricultura	40,1
2	Agricultura Irrigada	0,7
3	Cerrado	26,2
4	Área degradada	1,4
5	Reflorestamento	0,6
6	Floresta	0,7
7	Caatinga	29,3
8	Água	1,0

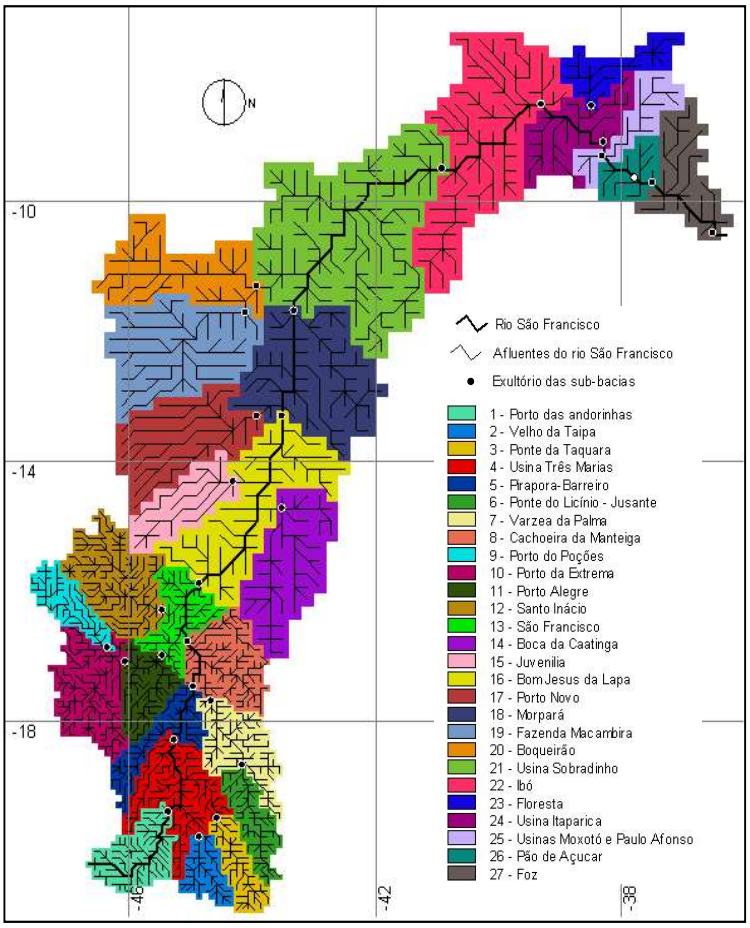

Figure 2.3.13. *Sub-basins for MGB-IPH model in São Francisco basin. 10km resolution until sub-basin 13 and 20km resolution downstream sub-basin 13.*

Table 2.3.5. *Sub-basins areas for MGB-IPH model in São Francisco basin*

Sub-bacia	Posto Fluviométrico	Rio	Área de Drenagem (km^2)
01	Porto das Andorinhas	São Francisco	13.867
02	Velho da Taipa	Pará	7.329
03	Ponte da Taquara	Paraopeba	8.729
04	Usina Três Marias	São Francisco	50.784
05	Pirapora-Barreiro	São Francisco	62.089
06	Ponte do Licinio - jusante	Das Velhas	10.637
07	Várzea da Palma	Das Velhas	26.406
08	Cachoeira da Manteiga	São Francisco	106.749
09	Porto dos Poções	Preto	9.407
10	Porto da Extrema	Paracatu	30.100
11	Porto Alegre	Paracatu	41.453
12	Santo Inácio	Urucuia	23.860
13	São Francisco	São Francisco	183.839
14	Boca da Caatinga	Verde Grande	30.089
15	Juvenilia	Carinhanha	16.312
16	Bom Jesus da Lapa	São Francisco	271.635
17	Porto Novo	Corrente	31.320
18	Morpará	São Francisco	346.825
19	Fazenda Macambira	Grande	40698
20	Boqueirão	Grande	70866
21	Usina Sobradinho	São Francisco	503.937
22	Ibó	São Francisco	564.658
23	Floresta	Pajeú	12.275
24	Usina Itaparica	São Francisco	596.495
25	Usinas Paulo Afonso e Moxotó	São Francisco	609.233
26	Pão de Açúcar	São Francisco	608.900
27	Foz	São Francisco	638.560

9. Method:

The calibration of the São Francisco River was similar to the Sapucaí River basin. The calibration assessment was performed visually, through subjective analysis of the calculated and observed hydrographs, and with the use of objective functions to measure the calibration performance. Validation was performance using Nash-Sutcliffe coefficient of calculated and observed flows (NS), Nash-Sutcliffe coefficient of the calculated and observed flow logarithms (NSLog) and relative error of the total volume of the hydrograph (ΔV). 27 sub-basins were calibrated for the periods from 01/01/1980 to 31/12/1989.

10. Results:

The results showed in the regions of the Upper and Middle São Francisco the MGB model a better performance compared to the regions of the sub-medium and low, as they are semi-arid regions and with fewer data available for calibration. The general performance of the model is presented Table 2.3.6, and Figures 2.3.14 and 2.3.15 shows the discharge simulation for sub-basins 1 and 21.

Table 2.3.6. *Sub-basins areas for MGB-IPH model in São Francisco basin.*

SUB-BACIA	POSTO FLUVIOMÉTRICO	NS	NSLog	ΔV (%)
1	Porto das Andorinhas	0.862	0.955	2.312
2	Velho da Taipa	0.847	0.795	9.365
3	Ponte da Taquara	0.740	0.802	-1.631
4	UHE Três Marias	0.898	0.861	5.152
5	Pirapora-Barreiro	0.941	0.911	-0.001
6	Ponte do Licínio - Jusante	0.739	0.833	3.916
7	Várzea da Palma	0.847	0.907	0.656
8	Cachoeira da Manteiga	0.918	0.927	-0.430
9	Porto dos Poções	0.787	0.809	-0.932
10	Porto da Extrema	0.921	0.868	3.668
11	Porto Alegre	0.898	0.882	3.509
12	Santo Inácio	0.772	0.800	0.281
13	São Francisco	0.960	0.937	5.225
14	Boca da Caatinga/Gado Bravo	0.916	0.351	0.853
15	Juvenília	0.876	0.860	0.197
16	Bom Jesus da Lapa	0.912	0.916	9.671
17	Porto Novo	0.715	0.703	0.129
18	Morpará	0.905	0.851	15.581
19	Fazenda Macambira	0.845	0.860	0.292
20	Boqueirão	0.791	0.779	-7.505
21	UHE Sobradinho	0.869	0.658	15.785
22	Ibó	0.899	0.741	11.677
23	Floresta	0.111	-0.973	-56.352
24	UHE Itaparica/Luiz Gonzaga	0.885	0.697	13.161
25	UHE Paulo Afonso/Moxotó	0.899	0.766	0.979
26	Pão de Açúcar	0.995	0.980	-0.867
27	Foz	0.974	0.925	1.710

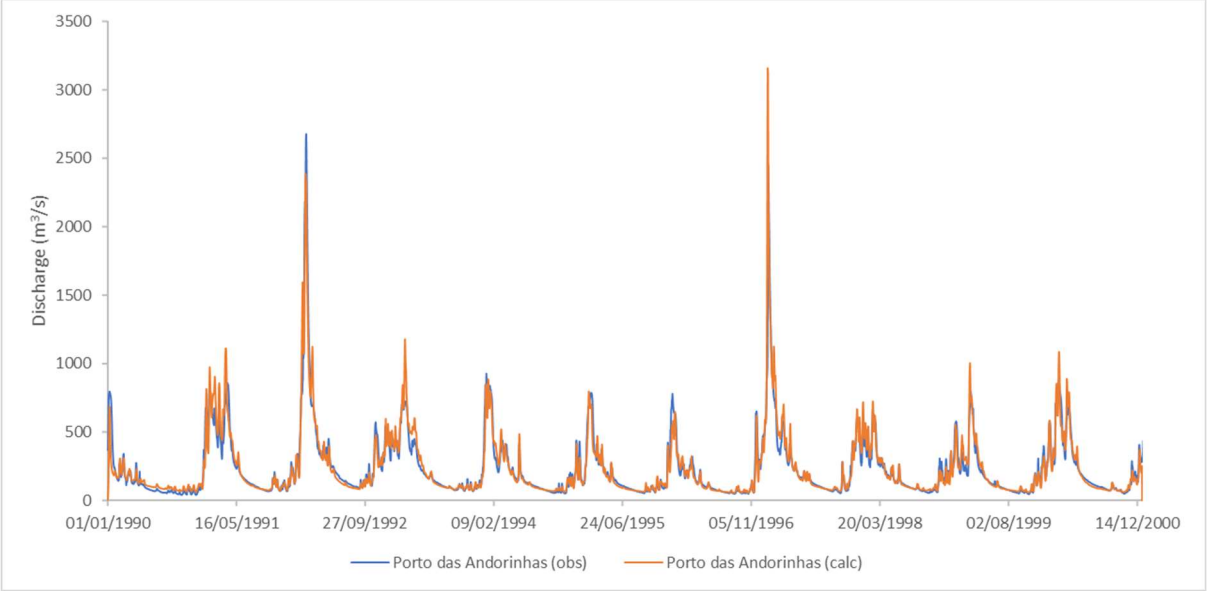

Figure 2.3.14. *MGB-IPH model calibration for Porto das Andorinhas (Sub-basin 1).*

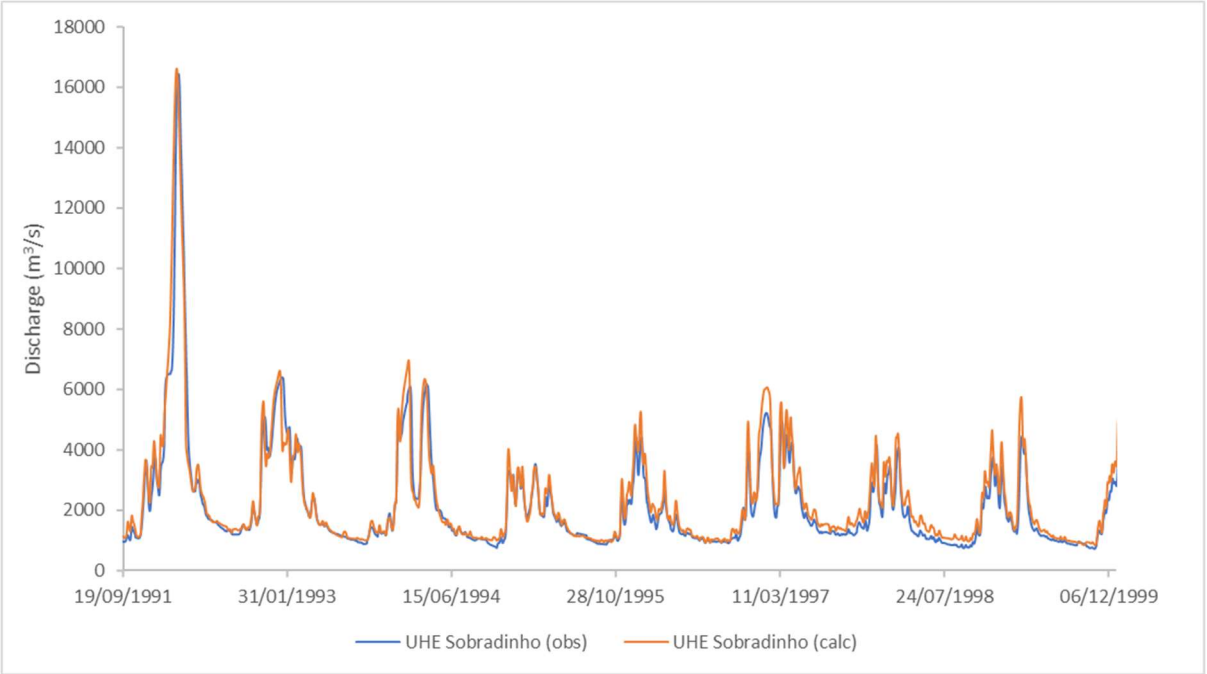

Figure 2.3.15. *MGB-IPH model calibration for Sobradinho Dam (Sub-basin 21).*

2.4 WP4.4 Rivers Mundaú and Paraíba do Meio (BR)

1. Case study no.: 4.4
2. Location:, Eastern Northeast Brazil (ENEB)
3. Country: Brazil
4. Domain size: 7,283 km^2
5. Case study area: Mundaú and Paraíba do Meio River basins

6. Description of hydrological (and other) pressures:
The Alagoas (BR) case study comprises two medium sized river basins, Mundaú and Paraíba do Meio (Fig. 2.4.1). Since the mid-1960s, the region has experienced at least eight extreme flash flood events

which have led to fatalities and substantial economic losses. The case study strives to develop a short-term flood forecasting with probabilistic flood maps that makes use of existing technologies in the basins (weather radar, automatic gauging stations). This includes hydrological reports with alerts based on water level and a web system for flood prediction.

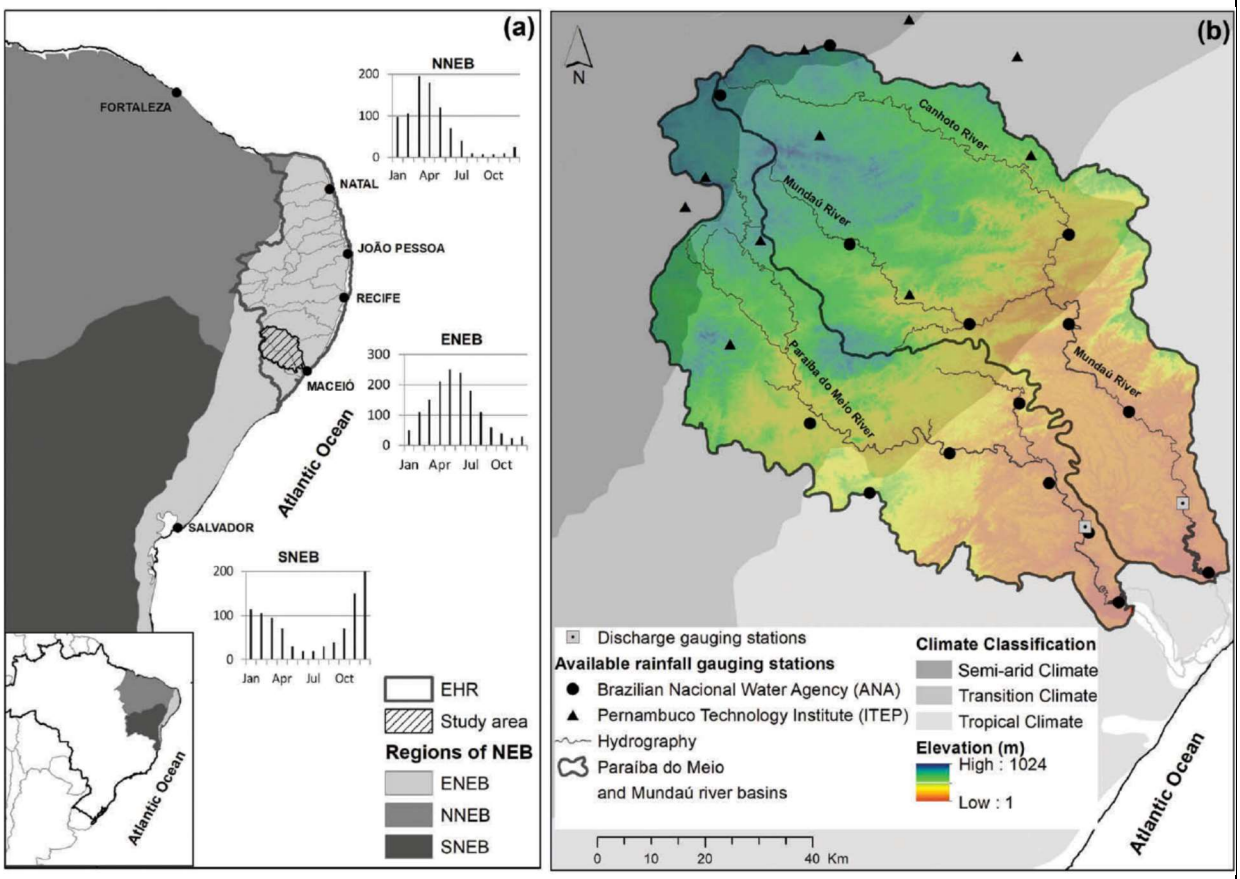

Figure 2.4.1. *Mundaú and Paraíba do Meio river basins.*

7. Local observations collected:

It was selected five flow data stations and 16 precipitation stations in the Mundaú and Paraíba do Meio river basins from the Brazilian Water Agency (ANA) database (http://www.snirh.gov.br/hidroweb/). The data selection was based on the period with the better stations distribution thorough the basins and the more significant data availability (years between 1990 and 2015).

Besides, for the regions where it had a low data availability, mainly at the upstream of the basins, it was used the interpolated daily gridded meteorological dataset published by Xavier et al. (2016).

8. Model:

The MGB-IPH consists of a distributed hydrological model that simulates the land phase of the hydrological processes by means of physical and conceptual relations. The MGB-IPH use small catchments (mini basins) to divide the watershed, and the Hydrological Response Unit approach (HRU) in order to reduce the number of model parameters and required input data. The model is composed of four modules: soil water balance, evapotranspiration, flow (surface, sub-surface and subterranean), and flow propagation in the drainage network. The parameters of the model are divided into fixed and calibrated ones and their values are defined based on local characteristics such as land use, topography, vegetation cover, and soil type.

The hydrological discretization was obtained using the digital elevation model from the SRTM (Shuttle Radar Topography Mission). The Mundaú basin has been divided into 157 mini basins and five sub-

basins, while Paraíba do Meio has been divided into 145 mini basins and five sub-basins. The land cover and soil types were defined using the HRU product defined by Fan et al. (2015) for the whole of Southern America.

9. Method:

Manually calibration of the MGB-IPH model for both Mundaú and Paraíba do Meio river basins. The model was calibrated using the flow data observation for a period of 17 years, from 01/01/1993 to 31/12/20019, and it was validated for five years of flow data observation, from 01/01/2010 to 31/12/2014. To calibration process was based on four coefficients, Nash-Sutcliffe, Nash-Sutcliffe of the logarithms, Kling-Gupta, and volume error. Moreover, it was used the visual assessment by the comparison between the hydrographs and the duration curves of the observed flow and the simulated flow to support the calibration process.

10. Results:

Examples of results from the MGB-IPH model are given in Figures 2.4.2-2.4.4. An overall good performance is attained for Mundaú river (Figure 2.4.2) although the observed extreme high and low flows are not fully captured, as exemplified by the underestimated event in 1997 (Figure 2.4.3). Also in Paraíba do Meio river, extremes are not fully captured, most clearly for low flows (Figure 2.4.4).

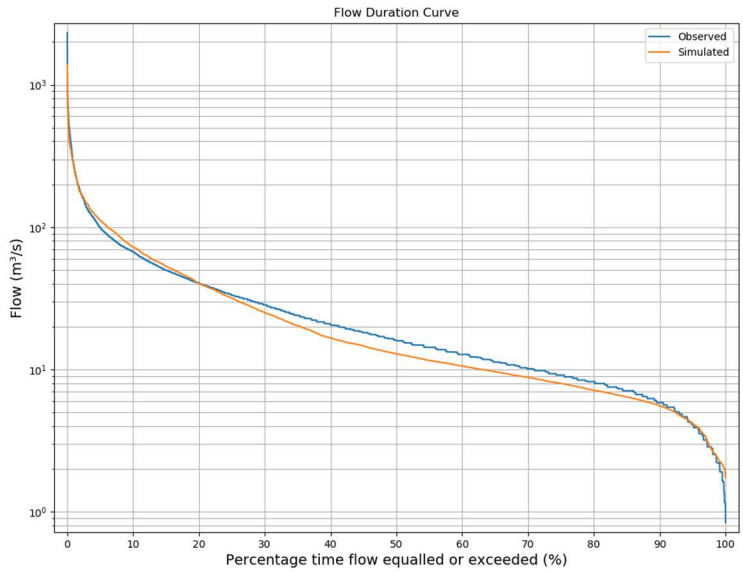

Figure 2.4.2. *Observed and simulated Flow Duration Curve for Mundaú river.*

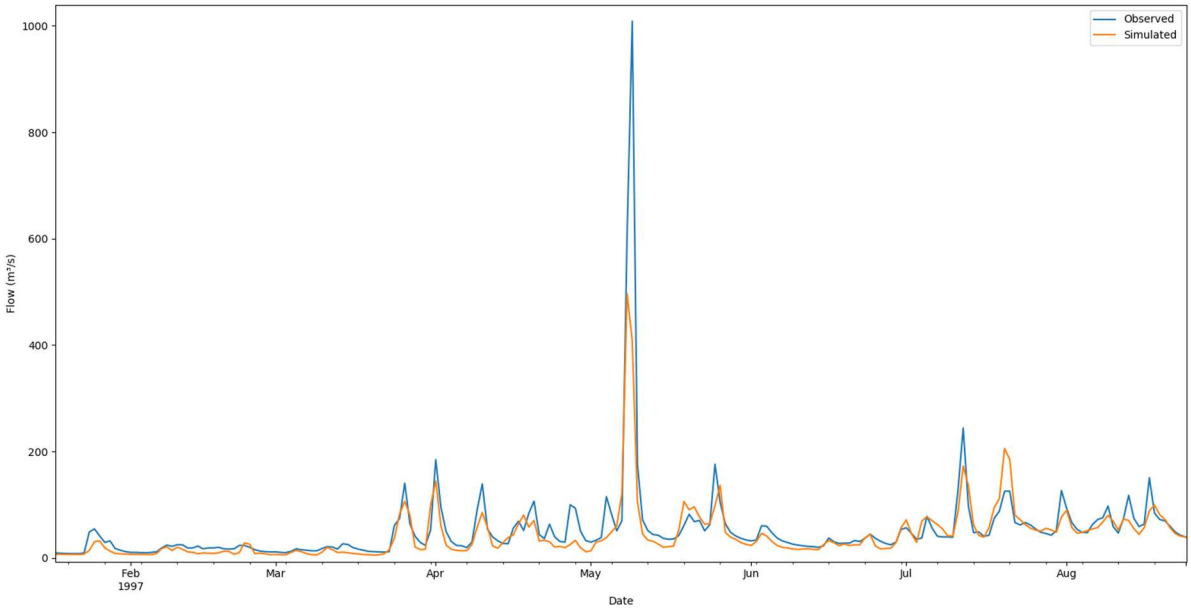

Figure 2.4.3. *Observed and simulated discharge for Mundaú river in 1997, including a very extreme event in May.*

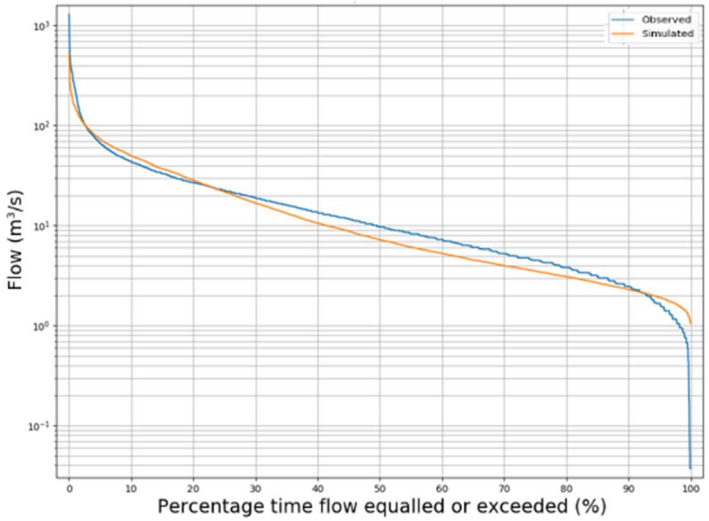

Figure 2.4.4. *Observed and simulated Flow Duration Curve for Paraíba do Meio river.*

2.5 WP4.5 Xinjiang (CH)

1. Case study no.: 4.5
2. Location: Xinjiang
3. Country: China
4. Domain size: 1.6 million km^2
5. Case study area and catchments for hydrological modelling:
Xiehela and Shaliguilanke catchment

6. Description of hydrological (and other) pressures:
The Xinjiang Uyghur Autonomous Region is the largest administrative region in China with geography and climate uniqueness. It is the most remote area from oceans on the earth and water are extremely valuable. The Urumqi River is one of the main rivers in the Xinjiang Uyghur Autonomous Region. The

Urumqi River is 214.3 km long and has its sources from the northern slopes of the Tianshan Kalawucheng Mountains, which is the largest mountains in central Asian and crosses four countries. The Urumqi River goes through the city of Urumqi, which is the capital of the Xinjiang Uyghur Autonomous Region and provides water to domestic and industrial needs for more than 2 million people in the city. Additionally, human activities consumer much more water than before after 1950s. More than 50% of river water irrigates farmlands. Effects of human activities has expanded to all the watersheds and all seasons. Moreover, given the current irrigation and cropping practice and a trend of expansion in irrigation area (Huang et al., 2018), the water scarcity may be cascaded further down, limiting the social and economic activities in the downstream area (Dadson et al., 2017). Water plays a significant role for important sectors, e.g. agriculture, water supply and hydropower production. Without supplementary water resources, seasonal water scarcity may pose a severe constraint on agriculture production, which in turn may harm the farmers, about 70% of the local population (Wang, 2006).

There are 20 000 glaciers in the Xinjiang Uyghur Autonomous Region, and they count half glaciers in China. These glaciers are very small and locates sparsely. They are very vulnerable to global warming and they are important supplementary water resources to precipitation. Since the 1950s, the glaciers have retreated by 21% to 27% as a consequence of climate change in the the Toshkan catchment and the Kumarik catchment while at the time domestic, industrial and agricultural water demand for has increased. There is a clear and urgent need to find a balance in water usage between human activities and natural system and to investigate how climate change will affect water availability at different scales. The case study aims to assess the impacts of projected climate change on glacier volume and area, available water resources, runoff seasonality, drought and hydropower potential. Water resources management strategies will be assessed.

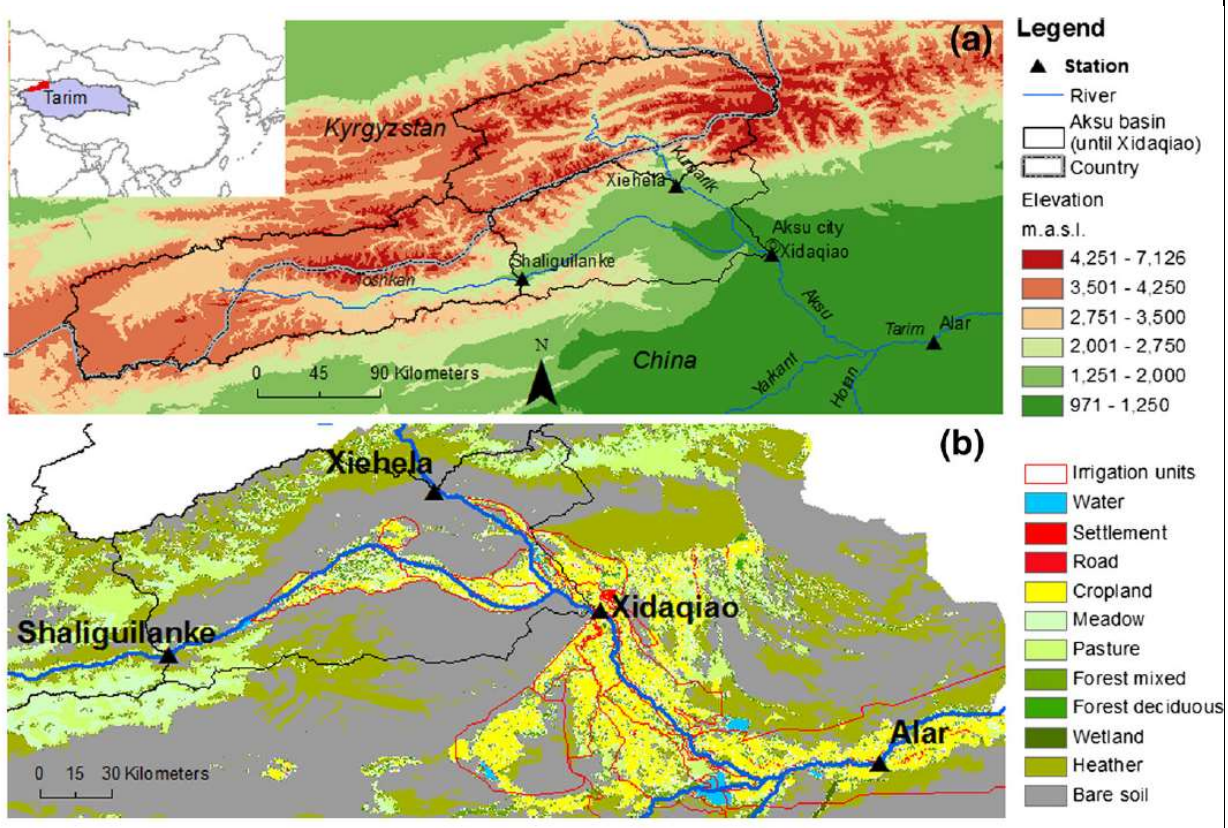

Figure 2.5.1. *Digital elevation of the Aksu basin (a) and land use of the lower part (Huang et al., 2015). The hydrological simulation area is above the Xiehela and Shaliguilanke stations. Runoff from these two catchments is the main source of water resources for the downstream irrigation units.*

7. Local observations collected:

The following data have been collected for the work in WP4.5:

- Daily Precipitation: APHRODITE V1901 1998-2015
- Daily mean temperature: APHRODITE V1808 1961-2015
- Daily discharge at the Xiehela station: 1980-1989
- Monthly discharge at the Xiehela station: 1956-2013
- Monthly discharge at the Shaliguilanke station: 1956-2004

8. Model:

The HBV model dates back to the 1970s, and it is initially developed for flood forecasting in Sweden (Bergström, 199576). It is later being used in more than 80 countries for operational flood forecasting, water resources management as well as a hydrological tool for scientific research (Lindström et al., 1997; Li et al., 2015). The main routines are snow accumulation and melting, evapotranspiration, and runoff generation. Precipitation falls as snow if the temperature is below a threshold, and snow melting is calculated by a degree method. Evapotranspiration occurs both at the vegetation canopy and the soil. Both are temperature based. Groundwater is conceptualized by two non-linear parallel reservoirs. The HBV model used in this study is a grid version first published by Beldring et al. (2003). Additional detailed information on the HBV model can be found in the references (Beldring et al., 2003; Li et al., 2014; Li et al., 2015).

The grid-based HBV model is setup for the catchments above the Xiehela and Shaliguilanke stations. The spatial resolution is 1 km with a uniform parameter set for the whole catchment and spatially distributed precipitation and temperature inputs.

9. Method:

Two versions of the HBV model have been set up and calibrated for the Xiehela Catchment, one with a daily and one with a monthly time step, to be used for pressure-specific similation and analysis.

As seen from the Local observations collected, the overlap period of discharge and climate inputs is from 1998 to 2013 for the Xiehela catchment and 1998 to 2004 for the Shaliguilanke catchment. Therefore, the HBV model was cross calibrated and validated against monthly discharge. The calibration and validation periods are shown in Table 2.5.1. Considering model outputs will be used for estimating of flood in the later stage of this project, the HBV model runs at the daily timestep in addition to the monthly timestep. Additionally, the HBV model is validated on the whole simulation period.

Table 2.5.1. *Overview of cross calibration and validation periods.*

Catchment	Calibration	Validation1	Validation2
Xiehela	1999-2008	2009-2013	1999-2013
	2004-2013	1999-2003	1999-2013
Shaliguilanke	1999-2002	2003-2004	1999-2004
	2001-2004	1999-2000	1999-2004

10. Results:

The HBV model works well on the two catchments according to the model performance criterion, Nash-Sutcliff efficiency (NSE) as shown in Table 2.5.2. All of them are above 0.75, which is usually a standard for good hydrological simulation. There is a small decline of NSE from calibration to validation in the Xiehela catchment, but no decline in the Shaliguilanke catchment. The hydrographs show that the HBV model underestimated the low flow during winter. The daily simulation provides more insights than the aggregated monthly discharge. For example, the year 2013 in the Xiehela

catchment is not a wet year according to the monthly discharge (Figure 2.5.4). However, at a daily timestep by the HBV simulation, the highest daily discharge happens in the year 2013.

Table 2.5.2. *Model performance (NSE) of the HBV model. The model was running at a daily timestep, but the NSE was calculated at a monthly timestep.*

Catchment	Calibration	Validation1	Validation2
Xiehela	0.86	0.81	0.85
	0.89	0.78	0.84
Shaliguilanke	0.81	0.81	0.81
	0.82	0.84	0.83

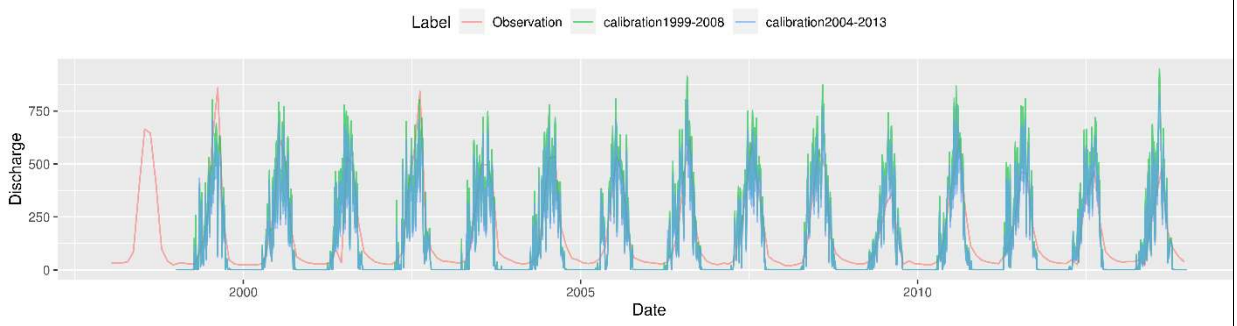

Figure 2.5.2. *Discharge at the Xiehela station.*

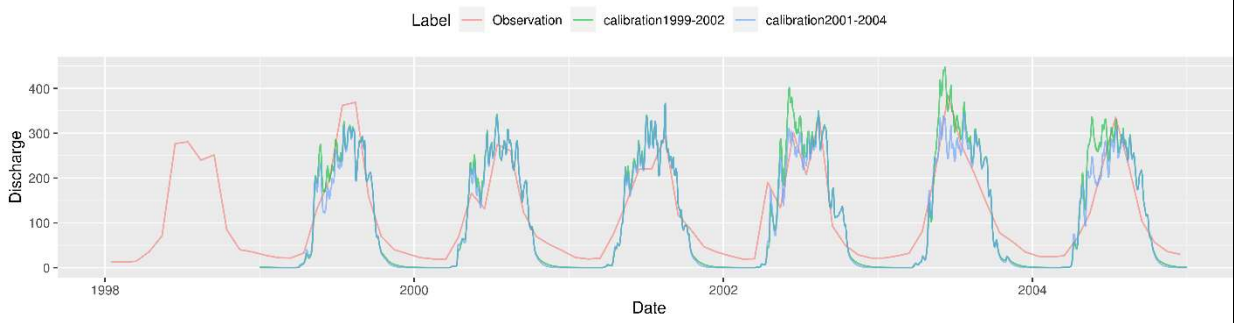

Figure 2.5.3. *Discharge at the Shaliguilanke station.*

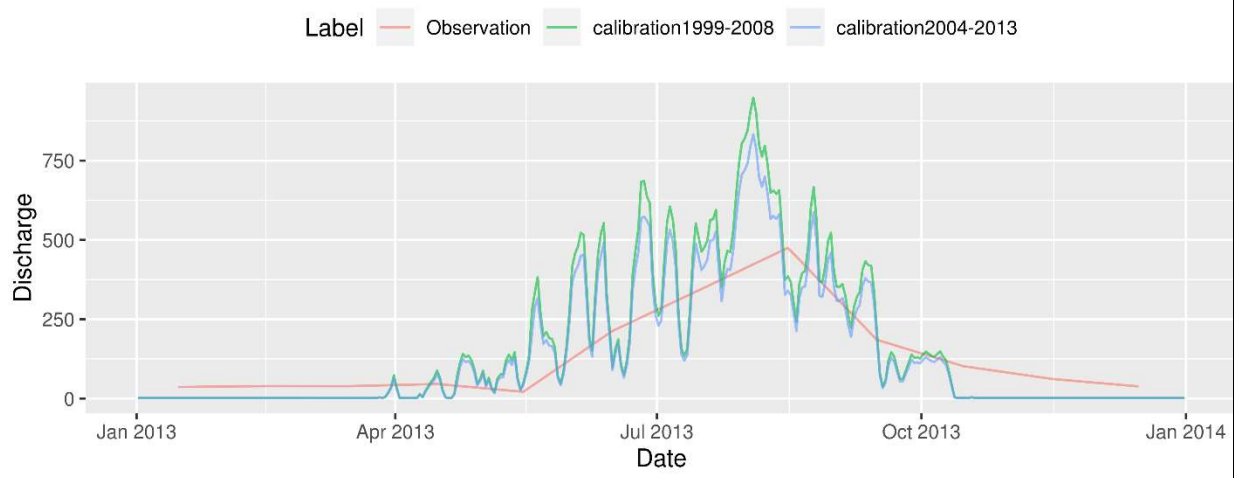

Figure 2.5.4. *Discharge at the Xiehela station for the year 2013.*

2.6 WP4.6 Western Norway (NO)

1. Case study no.: 4.6
2. Location: Western Norway
3. Country: Norway
4. Domain size: 34000 km^2
5. Case study area and catchments for hydrological modelling:
Totally 12 catchments with areas ranging from 45 km2 to 1 092 km^2 have been selected for hydrological modelling and analysis. The total area of the 12 catchments is 3 800 km^2. Furthermore, a spatially distributed hydrological model with 1 km^2 grid elements with be run for the entire domain size of 34 000 km^2.

6. Description of hydrological (and other) pressures:
Western Norway is a region dominated by steep terrain, high amounts of precipitation caused by extratropical cyclones migrating from west to east across the North Atlantic Ocean, a seasonal variation in snow cover and several glacier covered catchments. Many watersheds in this region have been developed for hydropower production, the dominating supply of electrical energy in Norway and a major source of electrical energy in Scandinavia. Heavy rainfall events can cause severe fluvial flooding and are projected to become more frequent in a warmer climate. At the same time, severe and prolonged water deficit periods have caused major problems in recent years with substantial impacts on hydropower production. The case study strives to provide improved tools to assess the impacts of climate and land use change on floods and droughts, including implications for hydropower production.

This region frequently experiences extreme precipitation events that produce flooding and landslides, causing considerable threats to human health, local communities and infrastructure. Current forest management practice in the region is dominated by clear-cutting and extensive clear-cut areas that increase hydrological risk in two aspects. Firstly, the steep terrain and frequent heavy rainfall events promote the formation of rainfall floods with short concentration times, and higher surface runoff contributions from clear-cut areas are likely to increase peak flood discharges. Secondly, clear-cut areas have a higher erosion potential with deteriorating effects on surface water quality. Given that both risks are tightly related to heavy precipitation events, which are projected to become more frequent in a warmer climate, adaptation strategies need to be developed that minimize hydrological risks from forest management.

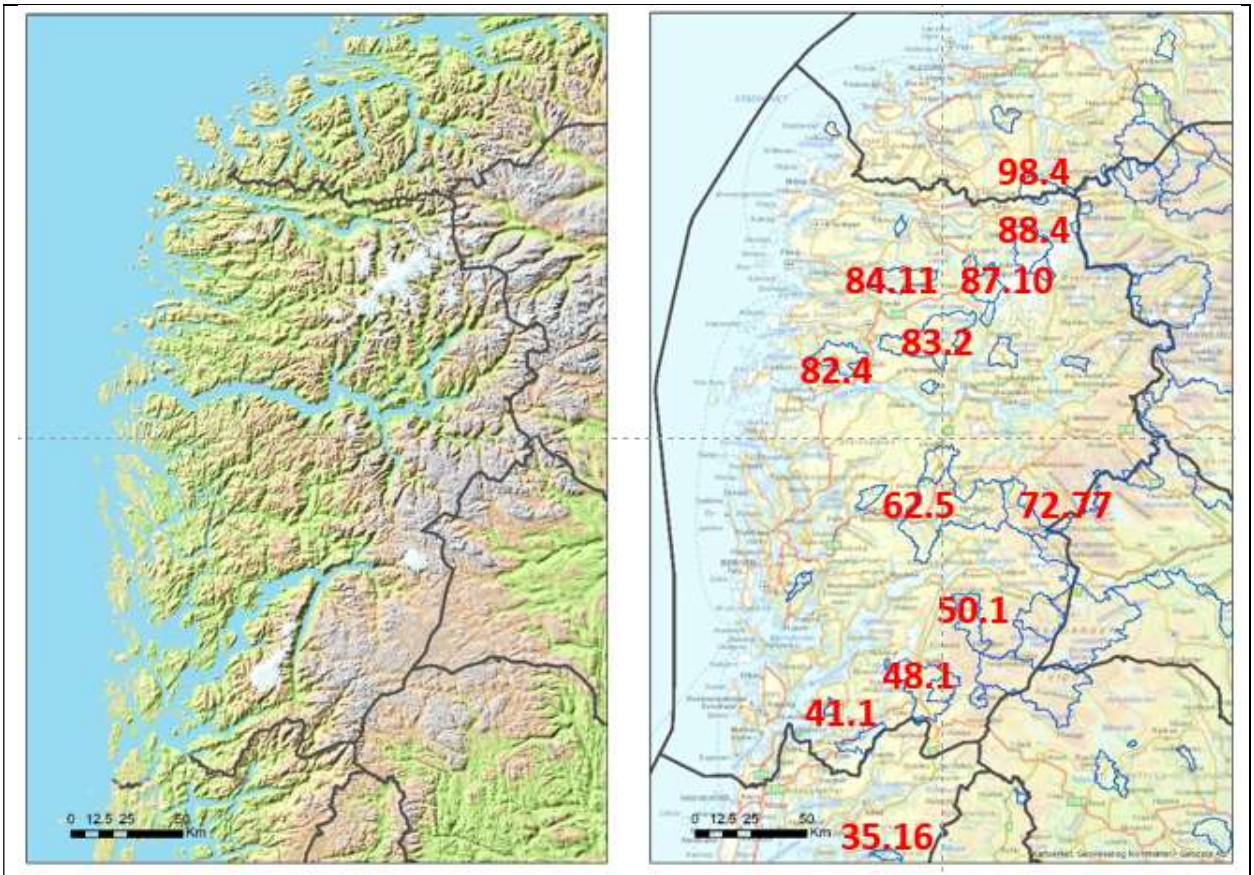

Figure 2.6.1. *Study domain in Western Norway (left) and catchments for modelling and analysis (right).*

7. Local observations collected:

Severe and prolonged water deficit periods have caused major problems in Norway in recent years. Low lake and groundwater levels threatened water supply in northern and western Norway in the winter of 2010, and electricity prices rose to unprecedented high levels as a result of the extreme low reservoir storages. Drought situations also occurred in 2018, 2006, 2003, and 1996. At the other end of the hydrologic scale, floods have caused significant challenges to society in form of damages to infrastructure, in particular in the autumn in 2014. Hydrological extremes for study area Western Norway for historical period of more than one hundred years have been identified by NVE and the results are presented in a report by Roald (2021). Information about observed floods is stored on the web site https://www.flomhendelser.no/.

Table 2.6.1. *Hydrological stations and streamflow time series.*

Station no. and name	River name	Time series id.	Observation period
35.16 Djupadalsvatn	Vormo	35.16.0.1001.1	1990-2019
41.1 Stordalsvatn	Etne	41.1.0.1001.1	1912-2019
48.1 Sandvenvatn	Opo	48.1.0.1001.1	1908-2019
50.1 Hølen	Kinso	50.1.0.1001.1	1923-2019
62.5 Bulken	Vosso	62.5.0.1001.1	1892-2019
72.77 Flåm bru	Flåmselvi	72.77.0.1001.0	1908-2019
82.4 Nautsundvatn	Guddalvassdraget	82.4.0.1001.0	1908-2019
83.2 Viksvatn	Gaularvassdraget	83.2.0.1001.1	1902-2019
84.11 Hovefoss	Nausta	84.11.0.1001.0	1963-2019
87. 10 Gloppenelv ved Bergheim	Breimsvassdraget	87.10.0.1001.0	1970-2019
88.4 Lovatn	Loenvassdraget	88.4.0.1001.1	1900-2019
98.4 Øye ndf.	Bygdaelva	98.4.0.1001.0	1900-2019

8. Model:

Table 2.6.2. *Catchments for HBV model.*

Station name	Area (km^2)	Elevation range (m a.s.l.)	Land use % (agriculture, bog, lake, forest, alpine vegetation, glacier)
Djupadalsvatn	45	338-1129	1, 4, 10, 33, 47, 0
Stordalsvatn	131	51-1294	3, 1, 10, 26, 60, 0
Sandvenvatn	470	87-1651	1, 1, 7, 21, 62, 8
Hølen	233	123-1686	0, 1, 8, 2, 88, 1
Bulken	1092	47-1602	3, 4, 5, 34, 54, 1
Flåm bru	263	28-1761	0, 1, 5, 12, 79, 3
Nautsundvatn	219	45-904	2, 1, 8, 39, 40, 0
Viksvatn	508	143-1635	2, 1, 10, 24, 58, 5
Hovefoss	234	20-1469	3, 6, 6, 27, 58, 0
Gloppenelv ved Bergheim	219	138-1823	3, 2, 3, 19, 55, 18
Lovatn	235	52-2071	0, 0, 5, 17, 44, 34
Øye ndf.	139	147-1848	3, 1, 5, 20, 67, 4

Streamflow records for the study catchments is available in the database system of NVE. Observed meteorological data with spatial resolution 1 by 1 km2 can be downloaded from the web site https://thredds.met.no/thredds/catalog/senorge/seNorge_2018/catalog.html.

Digital watershed and catchment data can be downloaded from the web site http://kartkatalog.nve.no/. Digital map data including terrain models and land use data can be downloaded from the web site https://www.geonorge.no/.

9. Method:

Two Four versions of the HBV model have been set up and calibrated for the study area in Wwestern Norway, one three with a daily and one with a 3-hour time step, to be used for pressure-specific similation and analysis.

1. Lumped model with 10 elevation bands and daily time resolution (Bergström, 1995; Sælthun, 1996)
2. Lumped model with 10 elevation bands and 3-hour time resolution (Beldring, 2008).
3. Spatially distributed model with 1 km^2 grid cells and Penman-Monteith potential evaporation (Huang et al., 2019)
4. Spatially distributed model with 1 km^2 grid cells and dynamic glacier retreat modelling (Li et al., 2015).

All the models were calibrated using the PEST Model-Independent Parameter Estimation and Uncertainty Analysis software package (Doherty, 2005) according to the procedure described by Beldring et al. (2003). No subcatchments were included in the model domains and water from all model computational elements, whether elevation bands or grid cells, were routed to the outlet of the catchments. Model parameters were determined by calibrating the model with the restriction that the same parameter values are used for all computational elements of the model that fall into the same class for land surface properties. This calibration procedure rests on the hypothesis that model elements with identical landscape characteristics have similar hydrological behaviour and should consequently be assigned the same parameter values. The computational elements should represent the significant and systematic variations in the properties of the land surface, and representative (typical) parameter values must be applied for different classes of soil and vegetation types, lakes and glaciers (Gottschalk et al., 2001). The model was calibrated using available information about climate and hydrological processes from all the catchments, and parameter values were assigned based on land use properties.

10. Results:

Figure 2.6.2. *Flood in river Opo downstream of catchment Sandvenvatn in October 2014. Photo by Jomar Bergheim (NVE).*

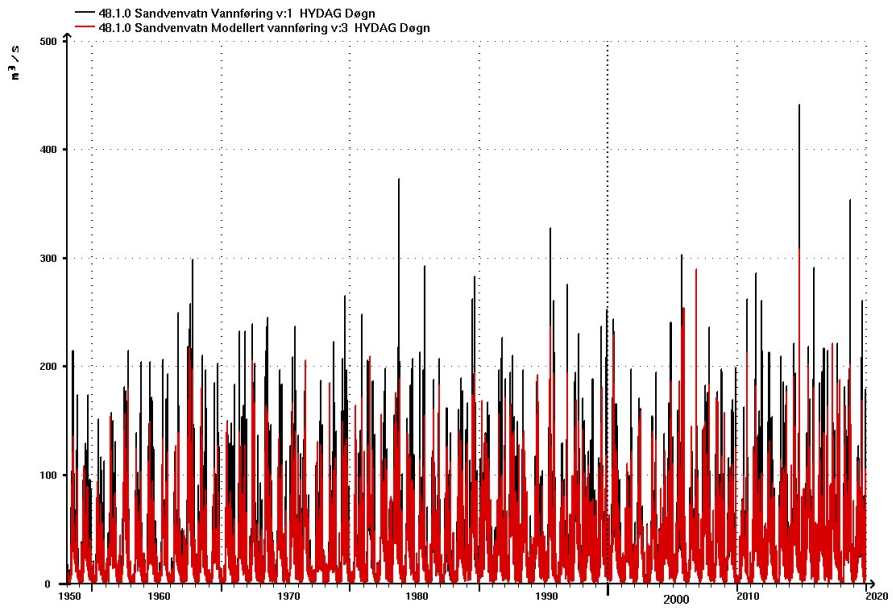

Figure 2.6.3. *Observed (black) and HBV model (red) daily streamflow from catchment Sandvenvatn for the period 1958-2019.*

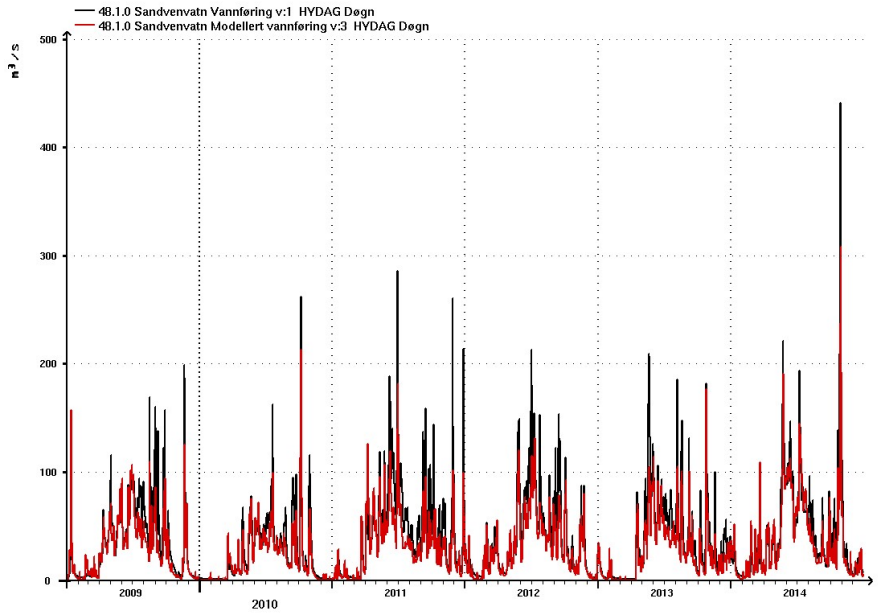

Figure 2.6.4. *Observed (black) and HBV model (red) daily streamflow from catchment Sandvenvatn for the period 2009-2014. Low flow periods occur in winter, snow melt floods in the spring and rain floods in the late summer and autumn. The flood in October 2014 has a return period of approximately 200 years.*

3. Future work

All the local models will be used in a joint evaluation with global/regional models, to assess the performance for different Deciusion Supprort Indicators (DSIs). In WP4.1, the assessment will include RCMs at different resolutions, from commonly globally available (44 km) to the highest possible local resolution (3 km). In WPs 4.2-4.6, the assessment will include different submodel versions based on the World-Wide HYPE model (see further deliverable D3.2).

4. References

Agência Nacional de Águas – ANA. Diagnóstico Analítico Da Bacia Do Rio São Francisco E Da Sua Zona Costeira. Brasília, ANA. 2003.

Beldring, S. 2008. Distributed element water balance model system. Norwegian Water Resources and Energy Directorate, Report no. 4/2008, 40 pp.

Beldring, S., Engeland, K., Roald, L.A., Sælthun, N.R., Voksø, A., 2003. Estimation of parameters in a distributed precipitation-runoff model for Norway. Hydrology and Earth System Sciences. 7, 304–316. http://dx.doi.org/10.5194/hess-7-304-2003.

Belušić, D. et al. (2020) 'HCLIM38: a flexible regional climate model applicable for different climate zones from coarse to convection-permitting scales', Geosci. Model Dev., 13(3), pp. 1311–1333. doi: 10.5194/gmd-13-1311-2020.

Bergström, S. 1995. The HBV model. In: Singh, V.P. (Ed.), Computer Models of Watershed Hydrology. Water Resources Publications, Highlands Ranch, 443-476.

COLLISCHONN, W. Simulação Hidrológica de Grandes Bacias. Porto Alegre: UFRGS. Tese (Doutorado em Recursos Hídricos e Saneamento Ambiental), Instituto de Pesquisas Hidráulicas da Universidade Federal do Rio Grande do Sul. 194p. 2001.

COLLISHONN, W.; ALLASIA, D. G.; SILVA, B. C.; TUCCI, C. M. The MGB-IPH model for large-scale rainfall-runoff modeling. Hydrological Science Journal, v.52, p.878-895. 2007.

Dadson, S., J. W. Hall, D. Garrick, C. Sadoff, D. Grey, and D. Whittington (2017). Water security, risk, and economic growth: Insights from a dynamical systems model, Water Resour. Res., 53, 6425–6438, doi:10.1002/2017WR020640.

Doherty, J., 2005. PEST: Model Independent Parameter Estimation: Fifth Edition of User Manual. Watermark Numerical Computing, Brisbane, Australia.. https://pesthomepage.org/.

Fan, F. M., Schwanenberg, D., Collischonn, W., and Weerts, A. (2015). Verification of inflow into hydropower reservoirs using ensemble forecasts of the TIGGE database for large scale basins in Brazil. J. Hydrol. Reg. Stud. 4, 196–227. doi: 10.1016/j.ejrh.2015.05.012

Gottschalk, L., Beldring, S., Engeland, K., Tallaksen, L., Sælthun, N.R., Kolberg, S., Motovilov, Y. 2001. Regional/macroscale hydrological modelling: a Scandinavian experience. Hydrological Sciences Journal, 46, 963-982.

Gustafsson, M., Rayner, D., Chen, D., 2010. Extreme rainfall events in southern Sweden: Where does the moisture come from? Tellus, Ser. A Dyn. Meteorol. Oceanogr. 62, 605–616. https://doi.org/10.1111/j.1600-0870.2010.00456.x.

Hanson, H., Larson, M., 2008. Implications of extreme waves and water levels in the southern Baltic Sea. J. Hydraul. Res. 46, 292–302. https://doi.org/10.1080/00221686.2008.9521962.

Hernebring, C., Milotti, S., Kronborg, S.S., Wolf, T., Mårtensson, E., 2015. Skyfallet i sydvästra Skåne 2014-08-31: Fokuserat mot konsekvenser och relation till regnstatistik i Malmö. VATTEN – J. Water Manag. Res. 71, 85–99.

Huang, S., Eisner, S., Magnusson, J., Lussana, C., Yang, X., Beldring, S. 2019. Improvements of the spatially distributed hydrological modelling using the HBV model at 1 km resolution for Norway. Journal of Hydrology 557:123585, https://doi.org/10.1016/j.jhydrol.2019.03.051.

Huang, S., Krysanova, V., Zhai, J., & Su, B. (20142015). Impact of Intensive Irrigation Activities on River Discharge Under Agricultural Scenarios in the Semi-Arid Aksu River Basin, Northwest China. Water Resources Management, 29(3), 945–959. https://doi.org/10.1007/s11269-014-0853-2.

Huang, S., Wortmann, M., Duethmann, D., Menz, C., Shi, F., Zhao, C., ... & Krysanova, V. (2018). Adaptation strategies of agriculture and water management to climate change in the Upper Tarim River basin, NW China. Agricultural Water Management, 203, 207-224.

Li, H., Beldring, S., Xu, C.-Y., 2014. Implementation and testing of routing algorithms in the distributed Hydrologiska Byråns Vattenbalansavdelning model for mountainous catchments. Hydrology Research. 45, 322–333. http://dx.doi.org/10.2166/nh.2013.009.

Li, H., Beldring, S., Xu, C.-Y., Huss, M., Melvold, K., Jain, S.K. 2015. Integrating a glacier retreat model into a hydrological model – Case studies of three glacierised catchments in Norway and Himalayan region, Journal of Hydrology 527, 656-667. http://dx.doi.org/10.1016/j.jhydrol.2015.05.017.

Li, H., Xu, C.-Y., Beldring, S., 2015. How much can we gain with increasing model complexity with the same model concepts? Journal of Hydrology. 527, 858–871. https://doi.org/10.1016/j.jhydrol.2015.05.044.

Lindström, G., Johansson, B., Persson, M., Gardelin, M., Bergström, S., 1997. Development and test of the distributed HBV-96 hydrological model. Journal of Hydrology. 201, 272–288. http://dx.doi.org/10.1016/S0022-1694(97)00041-3.

Lindström, G., Pers, C., Rosberg, J., Strömqvist, J. & Arheimer, B. (2010) Development and testing of the HYPE (Hydrological Predictions for the Environment) water quality model for different spatial scales. Hydrology Research 41.3–4, 295-319.

Paiva, R.C.D., Buarque, D.C., Collischonn, W., Bonnet, M.-P., Frappart, F., Calmant, S., Bulhoes Mendes, C.A., 2013b. Large-scale hydrologic and hydrodynamic modeling of the Amazon river basin. Water Resour. Res. 49, 1226e1243. http://dx.doi.org/10.1002/wrcr.20067.

PONTES, P. R. M.; FAN, F. M.; FLEISCHMANN, A. S.; PAIVA, R. C. D.; BUARQUE, D. C.; SIQUEIRA, V. A.; JARDIM, P. F.; SORRIBAS, M. V.; COLLISCHONN, W. MGB-IPH model for hydrological and hydraulic simulation of large floodplain river systems coupled with open source GIS. Environmental Modelling & Software, Amsterdam, v. 94, p. 1-20, aug. 2017.

Roald, L.A., 2021. Floods in Norway. NVE Report no. 1/2021. ISBN 978-82-410-2075-9. https://publikasjoner.nve.no/rapport/2021/rapport2021_01.pdf

Sælthun, N.R. 1996. The Nordic HBV model, Norwegian Water Resources and Energy Administration, Publication No. 7, Oslo, 26 s.

Strömqvist, J., Arheimer, B., Dahné, J., Donnelly, C. & Lindström, G. (2012) Water and nutrient predictions in ungauged basins: set-up and evaluation of a model at the national scale, Hydrological Sciences Journal, 57:2, 229-247.

Wang, Y., 2006. Local Records of the Akesu River Basin. Fangzhi publisher, China.

Xavier, A.C., King, C.W. and Scanlon, B.R. (2016), Daily gridded meteorological variables in Brazil (1980–2013). Int. J. Climatol., 36: 2644-2659. https://doi.org/10.1002/joc.4518